


HED 5/1. 12/23  
C.1

COLORADO STATE PUBLICATIONS LIBRARY  
HED5/1.12/23 local  
Middleton, John W/A cross-spectral stud  
  
3 1799 00003 7283

**"A CROSS-SPECTRAL STUDY OF THE  
SPATIAL RELATIONSHIPS IN THE  
NORTH PACIFIC SEA-SURFACE  
TEMPERATURE ANOMALY FIELD"**

by  
**John W. Middleton**



Environmental Research Papers  
COLORADO STATE UNIVERSITY  
Fort Collins, Colorado

Research on the environment constitutes an important component of the graduate programs pursued by a number of Colorado State University departments. The more noteworthy results of these research efforts are normally published in the conventional professional journals or conference proceedings, but in very much abridged form. ENVIRONMENTAL RESEARCH PAPERS has been established to provide a formal means of disseminating such CSU accomplishments in all significant details, in order that individuals concerned with related interests at other institutions may review a more comprehensive treatment of the research reported than is customarily available.

Price \$4.50 in USA

#### EDITORIAL BOARD

Professor Lewis O. Grant, Department of Atmospheric Science  
Dr. Judson M. Harper, Agricultural Engineering  
Dr. Elmar R. Reiter, (Editor), Department of Atmospheric Science  
Dr. David W. Seckler, Department of Economics  
Dr. Rodney K. Skogerboe, Department of Chemistry  
Dr. Evan C. Vlachos, Department of Sociology

Subscriptions and correspondence to these papers should be addressed to: Secretary of Environmental Research Papers, Department of Atmospheric Science, Colorado State University, Solar Village, Ft. Collins, CO 80523.

A CROSS-SPECTRAL STUDY OF THE SPATIAL RELATIONSHIPS IN THE  
NORTH PACIFIC SEA-SURFACE TEMPERATURE ANOMALY FIELD

by

John W. Middleton

Environmental Research Papers  
Colorado State University  
Fort Collins, Colorado

March 1980

No. 23

NOTICE

This report was prepared as an account of work sponsored by the United States Government. Neither the United States nor any of its agencies, nor any of their employees, nor any of their contractors, subcontractors, or their employees, makes any warranty, express or implied, or assumes any legal liability or responsibility for the accuracy, completeness, or usefulness of any information, apparatus, product or process disclosed, or represents that its use would not infringe privately owned rights.

# TABLE OF CONTENTS

	<u>Page</u>
TITLE PAGE . . . . .	i
ACKNOWLEDGMENTS . . . . .	iii
ABSTRACT . . . . .	1
I. Introduction . . . . .	2
II. Cross-Spectral Analysis and Study Design . . . . .	3
III. Grid Point Covariance Structure . . . . .	6
A. Regional Variations in Covariance Structure . . . . .	6
1. Midlatitude Region (North From 35N) . . . . .	6
a. Northwest (Westward from 165W) . . . . .	6
b. Northeast (East of 165W) . . . . .	9
2. Subtropical Region (Southward from 30N) . . . . .	10
a. Southeast (East of 170W) . . . . .	10
b. Southwest (West of 170W) . . . . .	10
3. Discussion of Regional Variations . . . . .	10
B. Transition Between Local-Scale and Basin-Scale Covariance Properties . . . . .	12
IV. Basin Scale Covariance Structure . . . . .	14
A. The Eastern North Pacific Seesaw . . . . .	17
B. Relations with the Southwestern North Pacific . . . . .	19
C. The Tropical Connection . . . . .	21
V. Summary and Discussion . . . . .	23
REFERENCES . . . . .	25



#### ACKNOWLEDGMENTS

The North Pacific sea-surface temperature data were supplied by T.P. Barnett of the Scripps Institution of Oceanography. Assistance in local data management and programming was provided by Dan Westhoff. The encouragement and support of this work by Professor Elmar R. Reiter is very much appreciated.

Some of the computations were performed at the Computing Facility of the National Center for Atmospheric Research at Boulder, Colorado. The grant of computing resources by NCAR is gratefully acknowledged. NCAR is supported by the Atmospheric Science Division of the National Science Foundation.

The research work reported in this paper was supported by NSF Grant ATM 78-17835 and by DOE Grant DE-AS02-76EV01340.

A CROSS-SPECTRAL STUDY OF THE SPATIAL RELATIONSHIPS IN THE  
NORTH PACIFIC SEA-SURFACE TEMPERATURE ANOMALY FIELD

by

John W. Middleton

Atmospheric Science Department  
Colorado State University  
Fort Collins, Colorado

ABSTRACT

Cross-spectral analysis is used to examine the dependence of the temporal covariation of sea-surface temperature (SST) anomalies at pairs of spatially separated points in the North Pacific on (1) the time scale of the variations, (2) the relative displacement of the points and (3) their location within the North Pacific basin. Spatial scales considered here range from 1000 kilometers up to the width of the basin. The study focuses on cross-spectral estimates for the interannual frequency band,  $0.125\text{--}0.75\text{ yr}^{-1}$  although estimates for three other bands spanning higher frequencies are also examined.

The study shows that, on interannual time scales, zonal and meridional coherence length scales are largest along the axes of the major mean North Pacific currents comprising the subtropical and subarctic gyres. The associated phase estimates uniformly indicate a small phase lead for the upstream point. These phase shifts appear to be relatively independent of separation within these regions suggesting that large-scale atmospheric forcing rather than advection is primarily responsible for the observed coherence. Some connections between the present cross-spectral study and one based on the stochastic modeling of grid point variance spectra are discussed.

Study of cross-spectral estimates for more widely separated points reveals three distinct regions whose variations have significant coherence with each other on interannual time scales. The out-of-phase relationship found between variations in the central North Pacific and those off the west coast of North America confirms the pattern appearing in the principal empirical orthogonal function of the sea-surface temperature anomaly field. The similarity is strongest in the interannual frequency band but appears as well in the higher frequency bands. Both of these regions are significantly coherent on interannual time scales with those in a third, less sharply-defined area in the vicinity of the subtropical temperature and salinity front in the southwestern North Pacific. Phase estimates show the variations in the southwestern region to have an apparent phase lag of  $\pi/4$  to  $\pi/2$  radians relative to those in the other regions.

Cross-spectral analysis of the relationships between SST variations in these areas and at Puerto Chicama, Peru reveals significant coherence on interannual time scales. The associated phase estimates show variations in the Northeastern North Pacific to have a slight lag behind those at Puerto Chicama while SST variations in the Central North Pacific are shifted by approximately  $\pi$  radians relative to those at Puerto Chicama. The hypothesis is advanced that the tropical-midlatitude teleconnection Bjerknes associated with the Southern Oscillation and El Niño is thus revealed in the low-pass filtered response of midlatitude SST to atmospheric forcing.

## I. INTRODUCTION

Interannual variations in seasonal climate are sufficiently pronounced as to be capable of disrupting human activity geared to the mean seasonal cycle in most regions of the world. The associated social and economic costs have spurred efforts to identify recurring patterns of atmospheric interannual variability which, if found, might be exploited to improve forecast skill. Such efforts indicate that the most apparent differences in seasonal atmospheric circulation statistics on interannual time scales are associated with the climatological "centers of action" (e.g. van Loon and Rogers, 1978). These large-scale, statistical (time mean) departures from axial symmetry in atmospheric circulation owe their existence to inhomogeneities in the lower boundary condition on the atmosphere related to surface topography (mountain ranges), albedo, and thermal capacity. The climatological centers of action undergo a distinct evolution during the annual cycle of insolation (U.S. Navy, 1956) due to variations the latter induces in the thermal content and albedo of the lower boundary surface. It is reasonable, therefore, to consider the possibility that some portion of the observed atmospheric interannual variability may be associated with long-term, nonseasonal variations in the boundary systems arising through the internal dynamics of these systems, through their individual interaction with the atmosphere, or through the coupling of different boundary systems by atmospheric transport processes.

The relatively well-documented interannual variation of the distribution of oceanic mixed layer thermal properties - particularly sea-surface temperature (SST) - provides an intriguing illustration of how the boundary conditions on the atmosphere vary from year to year. There has been much speculation on whether SST variability reflects merely the passive response of the mixed layer to low frequency atmospheric variations originating elsewhere or whether SST anomaly patterns significantly influence atmospheric circulation. If the former were the case, then the predictability of atmospheric interannual variability will be advanced little by a study of this coupling. Further insight into the nature of atmospheric interannual variability might, however, still be gained from studies of the SST distribution as the characteristics of the upper ocean as a low-pass filter of atmospheric variations become better known. If the latter were the case, then one might be able to forecast future states, even if SST variations were predictable only through persistence. It seems likely that the extent of mutual influence varies in both space and time.

The best established mutual relationship between sea-surface temperature and atmospheric circulation variations on interannual time scales appears in the tropical Pacific (Julian and Chervin, 1978). Here it would seem that the decreased stability and the increased water vapor flux into the atmosphere over anomalously warm water do measurably intensify the Hadley circulation. The associated increase in the easterly zonal wind stress reduces the sea-surface temperature in the eastern tropical Pacific by increasing upwelling. The appearance of colder water in the east enhances the zonal SST gradient hence the Walker circulation, while decreasing the meridional SST gradient in the east, thus diminishing the Hadley circulation. Apparently the enhanced Walker circulation is not sufficient to maintain upwelling and the zonal ocean pressure gradient, since warm water reappears in the east and the cycle begins anew.

The changes in angular momentum flux into the subtropical jet stream associated with fluctuations in Hadley circulation intensity may influence the strength of midlatitude circulation systems. Bjerknes (1966, 1969) describes evidence for a tropical-midlatitude teleconnection via the atmosphere in both the North Pacific and the North Atlantic longitude sectors. Case studies reveal a tendency for the Aleutian and Icelandic winter season lows to deepen when the trade winds in the Pacific and Atlantic sectors, respectively, are anomalously strong. Namias (1976) has stratified northern hemispheric circulation data based on the existence of abnormally warm or cold water at Puerto Chicama ( $8^{\circ}\text{S } 79^{\circ}\text{W}$ ). These results also suggest that the Aleutian low deepens and the winter westerlies strengthen when abnormally warm water appears in the eastern tropical Pacific during the northern hemisphere winter season.

While these results are suggestive, those of other studies are more ambiguous. In particular, Barnett (1977) has examined the cross correlation between time series of trade-wind anomaly empirical orthogonal functions (EOF's) and those of sea level pressure anomaly (SLP) over the North Pacific computed by Davis (1976). He finds an insignificant correlation between the principal EOF of sea level pressure anomaly and those of trade-wind anomalies. There does appear to be a significant relation between the first two EOF's of trade-wind u-component anomaly and the second EOF of SLP anomaly EOF with SLP slightly leading the u-component anomalies. It should be noted that the trade wind and SLP data sets overlap between  $20^{\circ}\text{N}$  and  $30^{\circ}\text{N}$  and that - unlike the principal SLP anomaly EOF - the second has a large amplitude in the east central Pacific in this latitude band as do the first two trade-wind u-component EOF's.

It may be hoped that either seasonal stratification of the data or low-pass filtering of the unstratified data would reveal more about tropical-midlatitude teleconnections in the Pacific sector. Support for the potential utility of low-pass filtering comes from previous studies of the Pacific SST structure. Weare et al. (1976) present patterns of empirical orthogonal functions for Pacific SST anomalies extending from  $55^{\circ}\text{N}$  south to include the eastern equatorial Pacific. The principal pattern depicts, in their opinion, the El Niño phenomenon as a Pacific basin scale phenomenon. The discussion provided in support is not in itself convincing since the significance of the North Pacific variations associated with this pattern is not demonstrated. However, there is a striking similarity between the principal pattern of Weare et al. (1976) north of  $20^{\circ}\text{N}$  and that of the principal EOF of North Pacific SST anomaly found by Davis (1976). Davis presents clear evidence that the time variation of the amplitude of this pattern is closely related to that of the principal empirical mode of sea level pressure anomaly over the North Pacific whose structure strongly suggests its relationship to variations in the Aleutian low. Statistically significant variations in the North Atlantic SST distribution associated with strengthening or weakening of the Icelandic low have been reported by Rogers and van Loon (1979).

Studies of the role of the midlatitude upper ocean in atmospheric interannual variability have generally attempted to discover temporal relationships between spatial patterns of variability in the fields characterizing both components. Namias (1978) has done much with the stratification of midlatitude SST distributions based on their proximity in time to

extreme cases of seasonal climate variation. Such studies are useful to the extent that the relationships which emerge are dynamically plausible and that examples on which the inferences are based number sufficiently many to permit confidence that the conclusions are unlikely to reflect only fortuitous sampling.

The studies of Davis (1976, 1978) and Weare et al. (1976) provide an alternative characterization of patterns of variability in the sea-surface temperature anomaly (SSTA) field through the use of empirical orthogonal functions (EOF's). The constraint of orthogonality (statistical independence) may lead some regions of variability to be divided among several EOF's and may obscure lag associations among regions which emerge only in the cross-correlation functions of the time series of EOF coefficients. Such potential problems are offset by other gains if one is primarily interested - as Davis is - in estimating the true skill of statistical prediction models. If, however, one is interested in deriving physical insight from the spatial structure of the principal EOF patterns one should estimate the statistical significance of spatial relations suggested by them. In the studies of Davis (1976) and Weare et al. (1976), the EOF's are constructed using the covariance matrix which includes all time scales from two months to the record length. The possibility that the character or intensity of spatial structures in SSTA vary with frequency is thus not examined. Cross-spectral analysis of the temporal relationship between SST variations at different grid points provides one means for examining these problems.

The relative importance of the processes which cause SST to change varies over the ocean reflecting in part the spatial inhomogeneity of atmospheric circulation, hence a clear recognition of the signature of these processes in observable SST variations would provide additional information on the large-scale air-sea interaction. Reynolds (1978) has attempted to distinguish regions where one-dimensional atmospheric forcing by local heat exchange is dominant over other processes, by fitting stochastic models to the variance spectra at grid points over the North Pacific. His results are suggestive and further motivate the cross-spectral analysis of relationships between grid points within regions to obtain further insight in the regionally predominant mechanisms of SSTA change. The unavailability of physically sound parameterizations of auto- and cross-spectra with which to make quantitative interregional comparisons limits the utility of such studies.

The following sections describe an empirical analysis of the covariance structure of the midlatitude North Pacific SSTA field based on the cross-spectral analysis of 32 years of monthly mean SST data provided on a  $5^\circ \times 5^\circ$  grid over the North Pacific by the Scripps Institution of Oceanography. A description of the design of the study and some of the considerations required for the interpretation of the estimates of cross-spectral parameters is given in the following section. The third and fourth sections describe empirical results and the fifth is a discussion of the results in the context of the large-scale air-sea interaction and contains suggestions for further work.

## II. CROSS-SPECTRAL ANALYSIS AND STUDY DESIGN

Cross-spectral analysis of spatially separated pairs of SSTA time series is the principal means employed herein to analyze spatial covariance structure. Technical descriptions of the method appear in numerous works on time series analysis (e.g. Bendat and Piersol, 1971 and Koopmans, 1974) hence remarks here are limited to those which aid the reader in interpreting results.

Quite briefly put, the product of cross-spectral analysis, the cross-spectral density, provides a spectral decomposition of the temporal covariance of two stationary time series. Its utility derives from the view that it provides the analyst of how the linear association between the two series varies with frequency. Since the cross-spectral density is a complex-valued function of frequency it is generally convenient to present the results of cross-spectral analysis in terms of a related pair of real functions. Several possibilities exist but the coherence and the phase are most convenient for the present study. A thorough discussion of the interpretation of these quantities appears in the book by Koopmans (Koopmans, 1974 § 5.5). It will suffice here to state that the coherence plays the role of a frequency dependent linear correlation coefficient between the two series. Its square gives the fraction of the variance in the chosen frequency band in one series which can be explained by linear regression with the other. The phase can be interpreted as the average phase lead or lag of realizations of one stochastic process over those of the other in the chosen frequency band.

Although in principal and in practice the computation of estimates of cross-spectral parameters is straightforward, the interpretation of results is not when - as is always the case - one is estimating the cross-spectral parameters from finite samples of the time series. Sampling distributions for both coherence and phase can be obtained if it is assumed that the time series are samples of multi-variate Gaussian processes (Koopmans, 1974 § 8.4). These results form the basis for statistical confidence tests concerning the estimators of coherence and phase which are employed in the following sections.

The principal disadvantage to analysis of gridded data in this way is that it may be difficult to digest the large amount of information which will be generated if a large number of grid-point pairs and frequency intervals are examined. Two factors moderate the problem encountered here. First, the SST data set is available in the form of averages over  $5^\circ \times 5^\circ$  regions and over a one-month time period. As a result, one finds that adjacent regions, especially those along latitude circles, are highly correlated on all but perhaps the shortest resolvable time scales. Thus, for example, it would be unnecessarily redundant to examine spatial structure by performing cross-spectral analysis for all possible pairs of grid points including all those adjacent along latitude circles. For this reason most of the analysis described in the next section has been performed on the subset of the Scripps data set at grid points shown in Fig. 1. Grid points along all latitude circles have

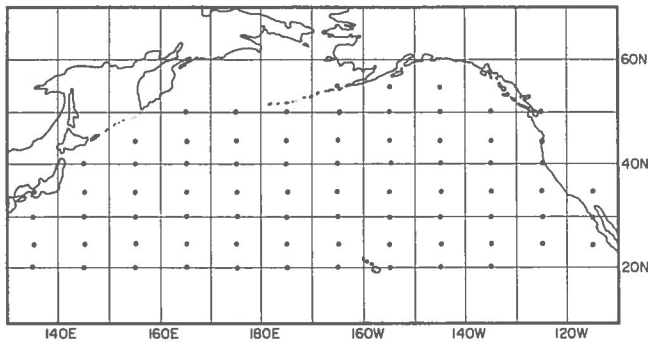


Fig. 1 Subset of Scripps data set used in this study.

been retained because, as might be expected, the meridional length scales of the second moment statistics of SSTA are much shorter than their zonal length scales over much of the North Pacific.

The spatial sampling strategy adopted here is to select *a priori* several plausible relative displacements and to then examine the cross-spectral estimates between all points so separated in the data set. The generally zonal structure of most atmospheric and oceanic fields - the latter away from the boundaries - and the meridional structure of the associated gradients suggest that the dependence of cross-spectral estimates on zonal and meridional separation be analyzed. The presence of boundary currents and the shape of the basin argue for some examination of separation dependence along directions oblique to the latitude-longitude coordinate axes. Separations along lines of slope  $\pm 0.5$  in the latitude-longitude coordinate system have been, somewhat arbitrarily, chosen for this purpose.

A second consideration limiting the useful information available here is the trade-off between the stability of cross-spectral density estimates and the resolution bandwidth of the estimates. Such a trade-off is unavoidable when spectral estimates are obtained from finite time series (Koopmans, 1974 § 9.3). Increasing the resolution bandwidth of the estimates reduces information available on frequency structure but increases the number of degrees of freedom determining the estimates hence their stability.

The recognition of regions of SSTA and their interrelations on the basis of cross-spectral estimates in a given frequency interval requires these estimates to have sufficient stability to insure that random errors do not obscure true regional differences. Whether or not this problem can be overcome depends both on the strength of the signal associated with the pattern and its bandwidth. With no *a priori* knowledge of either the strength or the bandwidth, it is advisable to obtain a low stability, narrow-band view of the spectral estimates as well as a high stability, broadband view. In this way both strong but narrow-band signals and weaker, broadband signals have the greatest chance of being detected.

The narrow-band view was obtained by computing ensemble-averaged estimates from the four non-overlapping blocks of eight years available in the thirty-two year record. Missing data at a grid point were filled by linear interpolation between reported values. A least squares linear trend was removed from

each eight-year segment and a cosine taper applied before Fourier analysis. Julian (1971) has demonstrated that the trend removal and tapering operations result in a 10% reduction in degrees of freedom per estimate. Each narrow-band estimate has a nominal 7 degrees of freedom (dof) and refers to a bandwidth of  $0.125 \text{ yr}^{-1}$ . To obtain a more stable, broadband view of the cross-spectral density, a straight running mean was applied to the ensemble averaged estimates for the coincident and quadrature spectra and the variance spectra. Broadband coherence and phase estimates were then computed from the frequency-averaged estimates. Table 1 lists the frequency bands used in the broadband analysis and an estimate of the degrees of freedom associated with each.

The lack of known narrow-band forcing and response mechanisms in the range of periods considered here (2 months to 8 years) leads one to expect that broadband relationships may be found. This contention is illustrated by graphs of coherence and phase estimates for the pair of regions centered at 165E, 40N and 175W, 40N presented in Figs. 2 and 3. The first figure shows the basic ensemble-averaged estimates, each having approximately 7 degrees of freedom. Dramatic fluctuations in both coherence and phase estimates as functions of frequency are apparent but are more likely to represent accidental features of the particular finite sample of the SSTA on which they are based than true narrow-band interrelationships between the data sets. One cannot resolve this ambiguity with certainty using any finite sample, hence other critical considerations must be made. Figure 3 portrays estimates involving the same points but with resolution bandwidth sacrificed for stability through frequency averaging as described above. The fact the hypothesis of zero coherence can be rejected at the 95% confidence level for all coherence estimates for frequency bands lower than  $0.8 \text{ yr}^{-1}$  suggests strongly that significant coherence is a property of the whole band. The decrease in coherence with increasing frequency seen in Fig. 3 is a general feature of the coherence estimates involving different data points examined here.

Given sufficient stability in the coherence and phase estimates, pattern can be expected in the spatial distribution of estimates obtained through the spatial sampling strategy described above. The statistical significance of apparent pattern features then should be considered. Whereas individual EOF patterns are determined both by the sample covariance estimates and the requirement of mutual orthogonality appearing in the eigenvalue problem, the features seen in the cross-spectral analysis here can be due only to real or accidental temporal associations between spatially separated points. The familiar *a priori* confidence levels for coherence and phase estimates provide only limited insight into the significance of spatial patterns of estimates arising from statistically dependent though spatially separated variations.

Table 1

Frequency Band ( $\text{Yr}^{-1}$ )	Degrees of Freedom (dof)	Critical Values for Zero Coherence Null Hypothesis			
		75%	90%	95%	99%
0.125-0.750	43	0.26	0.33	0.37	0.45
0.750-1.375	43	0.26	0.33	0.37	0.45
1.500-2.875	86	0.18	0.23	0.27	0.32
3.000-5.875	173	0.13	0.16	0.19	0.23



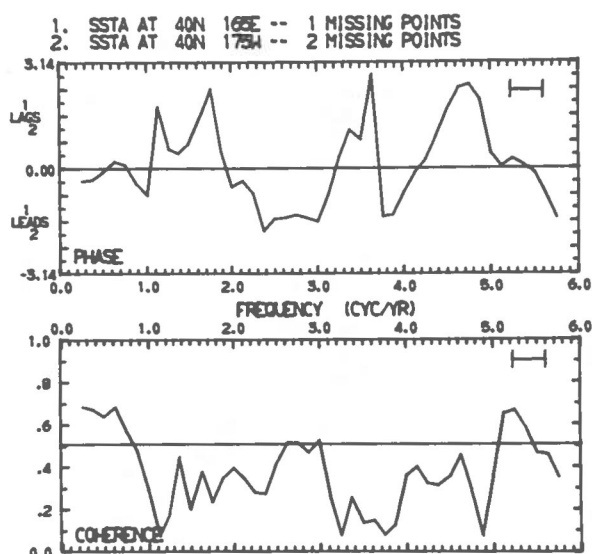


Fig. 2 Coherence and phase between 165E 40N and 175W 40N based on 7 dof per estimate.

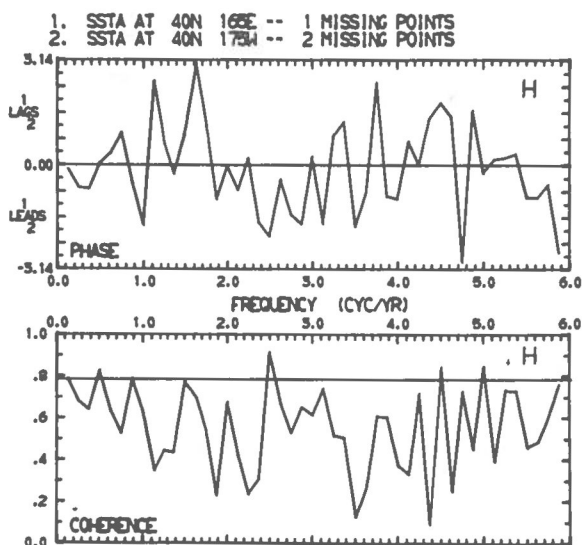


Fig. 3 Same as Fig. 2, but with 21 dof per estimate.

in a data field such as that of North Pacific SST. Where possible, especially in the definition of regions for the study of basin scale relationships, the degree of consistency of coherence and phase estimates between interior points is examined. Since

the possession of common modes of variability would seem a necessary condition for identifying a physical region. This does not, however, yield a quantitative measure of the statistical significance of regional interrelationships. Dynamical insight into the origins of SST variations may help resolve some questions but the complexity of the process makes it likely that some doubts will remain.

The seasonal variation in the strength and relative predominance of physical processes influencing the evolution of mixed layer temperature have potentially serious effects on the interpretation of studies based on the techniques of analysis of stationary time series. Although spectral peaks at the annual frequency and its harmonics can be greatly reduced by studying SST departures (anomalies) from climatological mean monthly values, the relationships among temporal variations at different locations may well vary as the forcing and response fields change with the seasons. On time scales less than one year it may be difficult to decide if apparent coherence between different points is largely due to relationships existing in one season or to actual relationships which are present in several seasons (though perhaps due to different mechanisms in different seasons). On the other hand, lack of significant coherence on these time scales may result from the existence of different relationships in different seasons. Thus the connection between dynamical processes and the spatial covariance structure for seasonally unstratified data on time scales of less than one year may be difficult to obtain convincingly.

The analysis of spatial relationships in SST having interannual time scales faces some of the ambiguities mentioned in the discussion of intraannual variation of SST anomalies. Are spatial relationships apparent on these time scales due to interannual differences in a particular season (or seasons) or are they related to shifts throughout the entire annual forcing cycle? The former might occur if the magnitude or persistence of patterns of SST variations depends on the season in which they are created. Seasonal stratification of the data provides an alternative and somewhat complementary view of interannual variability which may be required to characterize the underlying dynamical relations.

To provide additional perspective on the nature of interannual variations of the actual time series reflected in the low frequency cross-spectral estimates, low-pass filtered versions of some of the SST time series are presented. The family of least squares low-pass filters used here has been described by Bloomfield (Bloomfield, 1976 § 6.4). The cutoff frequency (approximate center of the transition band) has been chosen as  $0.78 \text{ yr}^{-1}$  ( $= 0.065 \text{ mo}^{-1}$ ) with the number of terms in the filter being generally either 49 or 97. Plots of the transfer functions for filters having this cutoff frequency and various numbers of terms (nonzero weights) appear in Fig. 4.

ERRATUM  
THE PLOTS IN FIGS. 2 AND 3 ARE INTERCHANGED.

SYMMETRIC LOWPASS FILTER  
LEAST SQUARES FIT TO IDEAL WITH CONVERGENCE FACTORS

NUM	CUTOFF	ITERMS
1	.0650	7
2	.0650	25
3	.0650	49
4	.0650	97

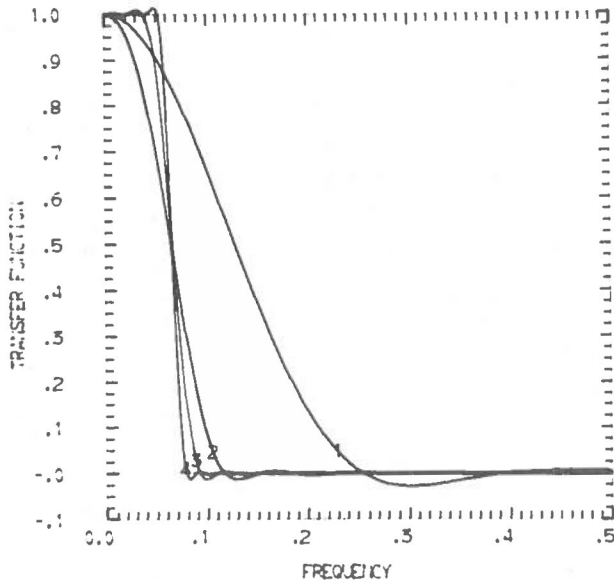


Fig. 4 Transfer function for the least squares low-pass filter described in § 6.4 of Bloomfield (1976). The abscissa is in units of the Nyquist frequency. The cutoff frequency is  $0.065 \text{ mo}^{-1} = 0.78 \text{ yr}^{-1}$ .

### III. GRID POINT COVARIANCE STRUCTURE

This section examines the behavior of cross-spectral estimates between pairs of grid points as relative displacement is varied from the smallest resolvable separations to those of the scale of the North Pacific basin. The picture which emerges features marked intraregional differences in the cross-spectral densities which become even more striking as basin scale separations are considered. In principal the characteristics of the local cross-spectral estimates within a region reveal something of the nature of the processes leading to the existence of the region. Much additional work on the parametric modeling of the influence of physical processes on SSTA cross spectra is required before a quantitative ordering of dominant processes within regions can be accomplished from empirical estimates such as those computed here.

The discussion of grid point cross-spectral estimates is presented in two parts reflecting the transition from intraregional to interregional properties which is apparent in these estimates as the separation between the sampled pairs increases. Subsection III.A attempts to portray how the relationship between temporal SSTA variations at nearby grid points varies with location in the North Pacific

basin. A qualitative description is presented of the relationship between the observed second-moment structure of the SSTA field and the climatological features of atmospheric and oceanic circulation in the Pacific sector as well as the spatial structure of variations about the climatological states when information is available. The appearance of interregional relationships in the grid point estimates as separation is increased is described in Subsection III. B.

Maps of cross-spectral estimates from all grid point pairs having a specified relative displacement are central to the following discussion. The estimates are located on the maps (e.g. Fig. 5) at the midpoint of the straight line joining the two points on the latitude-longitude grid. This convention is shown graphically in each figure. The magnitude of the coherence is indicated by the number of symbols (circles or triangles). The larger the number of symbols, the higher the significance level of the coherence estimate as shown in Table 2. The actual range of magnitudes of these estimates can be determined from Table 1 using the estimate of degrees of freedom stated on each map. The numbers appearing beneath the symbols are the estimates of phase given in radians in the interval  $[-\pi, \pi]$ . Negative values indicate that data set 1 of the pair leads data set 2 with the convention as to which data set is 1 and which 2 is stated in each figure.

Table 2

Symbols for Graphical Representation of Coherence Estimates

Symbol	Significance Level of Coherence Estimate
Blank	< 75%
•	75% - 90%
••	90% - 95%
•••	95% - 99%
••••	> 99%

#### A. REGIONAL VARIATIONS IN COVARIANCE STRUCTURE

This subsection describes the variation over the North Pacific basin of cross-spectral estimates for pairs of SST data points (see Fig. 1) separated by less than 2000 km. Striking differences are observed on these length scales which can be qualitatively related to large-scale differences in the overlying atmospheric circulation.

The presentation of this study is divided into three general parts. The first and second discuss the midlatitude region north of 30N and the subtropical region from 20N to 30N. The third presents an overview and a comparison with Reynolds's autospectral study of North Pacific SSTA (Reynolds, 1978).

##### 1. Midlatitude Region (Northward From 35N)

###### a. Northwest (Westward from 165W)

Westerlies prevail in all seasons in the overlying atmosphere (U.S. Navy, 1956), and the eastward flowing Kuroshio and Oyashio extensions are prominent in the upper ocean. Pronounced meridional SST gradients occur in the vicinity of 40N reflecting the

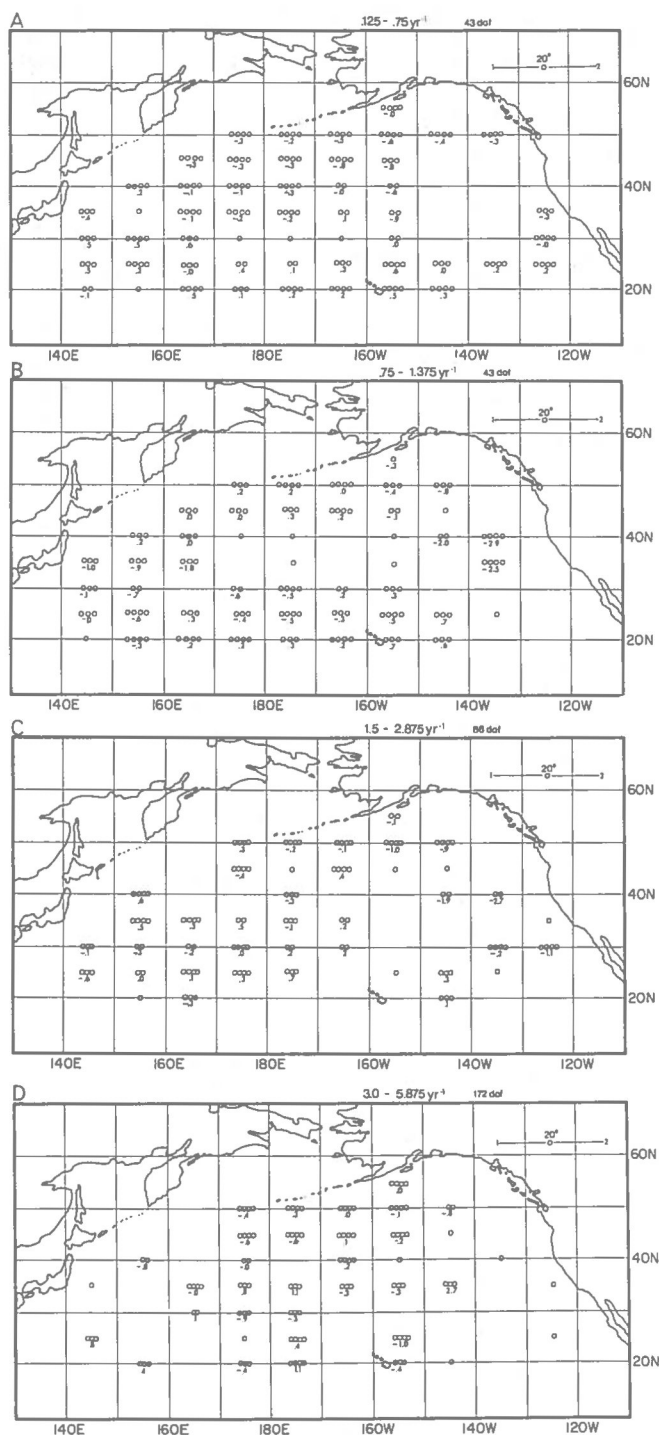


Fig. 5 Coherence and phase estimates in the frequency bands (a)  $0.125-0.75 \text{ yr}^{-1}$ , (b)  $0.75-1.375 \text{ yr}^{-1}$ , (c)  $1.5-2.875 \text{ yr}^{-1}$ , and (d)  $3.0-5.875 \text{ yr}^{-1}$  for all pairs separated by  $20^\circ$  longitude. Number of symbols reflects level at which a priori hypothesis of zero coherence can be rejected as indicated in Table 2. Numbers below symbols are phase estimates in radians, with negative value indicating dataset 1 leads data-set 2. Symbols and phase estimates are located at midpoint of line joining the latitude-longitude grid points of the two data sets.

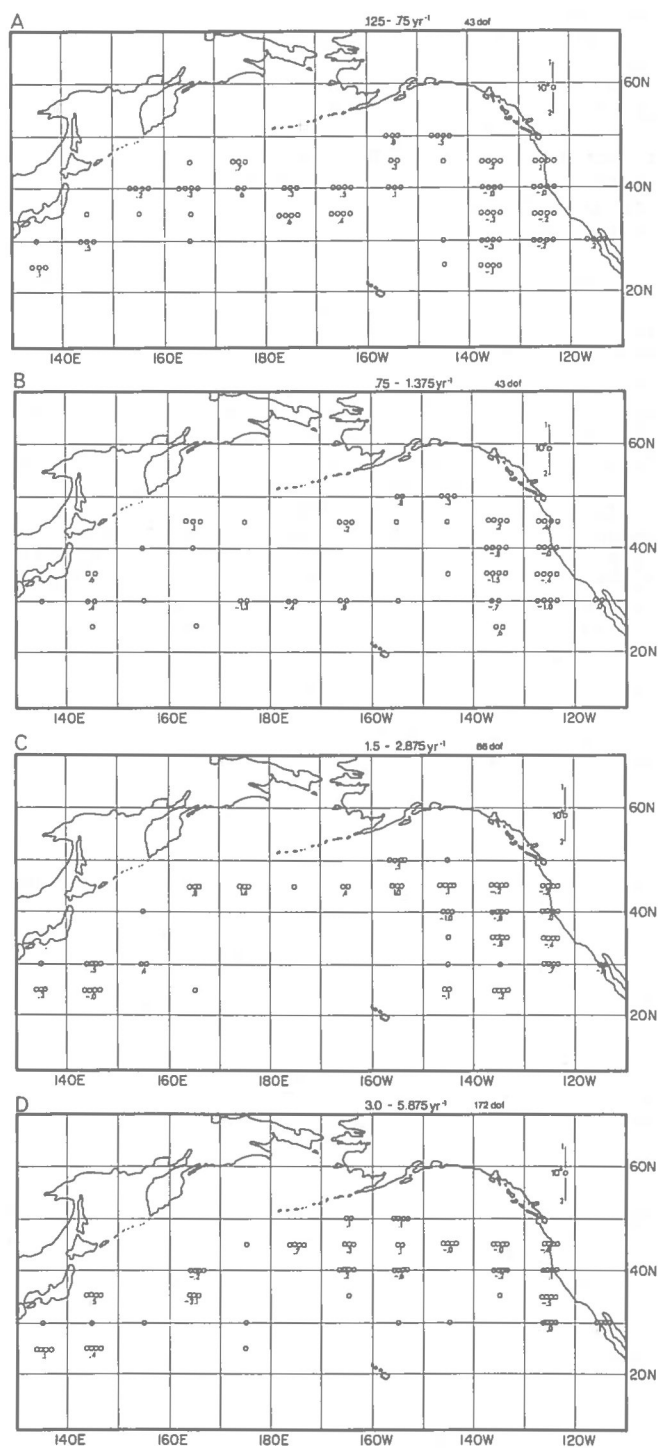


Fig. 6 Coherence and phase estimates in the frequency bands (a)  $0.125-0.75 \text{ yr}^{-1}$ , (b)  $0.75-1.375 \text{ yr}^{-1}$ , (c)  $1.5-2.875 \text{ yr}^{-1}$ , and (d)  $3.0-5.875 \text{ yr}^{-1}$  for all pairs separated by  $10^\circ$  latitude. For further explanatory remarks see Fig. 5.



convergence of the wind driven surface flow south of the zone of maximum westerlies. Viewing Figs. 5a and 6a it appears that this region is characterized, relative to others immediately to its south and east, by relatively large values for coherence on interannual time scales along latitude circles and between points along 35N and 45N. (The conventions employed in these and subsequent plots of cross-spectral estimates are described in the introductory paragraphs above and in the caption for Fig. 5.)

More specifically, the coherence between points separated by  $20^\circ$  longitude on, and north of, 45N between 165E and 145W is apparent (see Fig. 5) in all frequency bands considered. The phase estimates in the frequency band  $0.125\text{--}0.75\text{ yr}^{-1}$  are consistently negative indicating a tendency for a phase lead for the western point of the pair over the eastern one. Occasionally, as in 1959 and 1974, a systematic time lag of east over west is apparent in the low-pass filtered time series from 45N shown in Fig. 7. Phase estimates in the other frequency bands are more uniformly scattered about zero radians. Coherence between points separated by  $20^\circ$  longitude along 40N and 45N in the Pacific west of 175E appears most convincingly in the lowest frequency band,  $0.125\text{--}0.75\text{ yr}^{-1}$ . Phase estimates in this region are consistently small and negative which again suggests a phase lead for the west over the east. The lack of significant coherence in the higher frequency bands may be related to the influence of shorter time and smaller space scale oceanic processes on SSTA in the eastward extensions of the Kuroshio and Oyashio.

Along 35N west of 165W, coherence between points separated by  $20^\circ$  longitude is evident in all frequency bands. The consistent but small phase lead indicated for western points over eastern ones rarely appears as a time lag of eastern over western variations in the low-pass filtered SSTA plotted in Fig. 8. The existence of coherence on interannual time scales between pairs separated by  $30^\circ$  and  $40^\circ$  longitude in this region is indicated in Figs. 9 and 10. It is interesting that the phase estimates here again indicate a phase lead for the western point over the eastern one of about the same magnitude seen in Fig. 5 for separations of  $20^\circ$  longitude.

In the lowest frequency band (Fig. 6a) there is apparently significant coherence for meridional separations of  $10^\circ$  latitude involving points along 35N and 45N west of 165W and for points along 30N and 40N between 165W and the date line. The uniformly positive phase estimates here suggest variations in the south leading those  $10^\circ$  to the north. Comparison of low-pass filtered series along 45N (Fig. 7) and 35N (Fig. 8) and along the meridians 150E and 170E shown in Figs. 11 and 12, respectively, reveal several events (e.g. 1959, 1979) which have the temporal relationship suggested by the phase estimates. Only scattered evidence for significant meridional coherence in the higher frequency bands appears in Figs. 6b-d.

Coherence estimates (not shown) on interannual time scales between grid points separated by  $5^\circ$  latitude show a pronounced relative maximum for pairs along 35N and 45N between 165E and 165W. Estimates in the higher frequency bands reveal a relative minimum in the same region. This evidence, as well as that appearing in Fig. 6, suggests that the meridional coherence transverse to the Kuroshio (and Oyashio)

extensions is associated primarily with interannual time scales. Given the existence of active eddy processes in the Kuroshio extension, it seems likely that the lower values of transverse coherence and longitudinal coherence along 40N seen in the higher frequency bands reflect the dominance of the smaller scale oceanic processes on shorter time scales.

Unfortunately the evidence presented here does not, at the present time, yield conclusive insight into the processes responsible for the spatial coherence of SST variations in this region on interannual time scales. It seems probable, though, that the large zonal length scale for coherence and the meridional coherence between 35N and 45N are the result of the large-scale anomalous forcing of the mixed layer by interannual variations in the westerlies. Additional evidence for this suggestion is described in the course of this work.

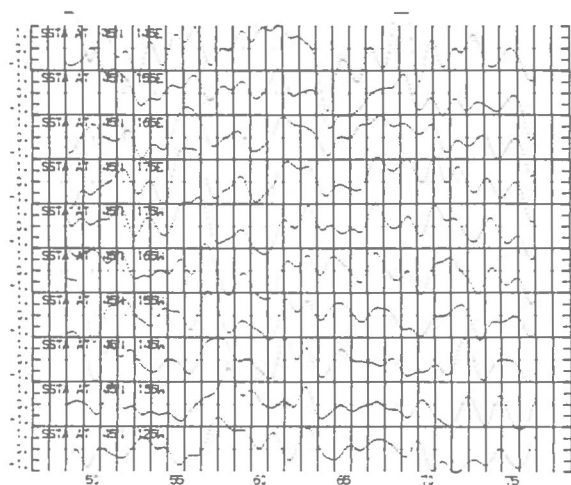


Fig. 7 Low-pass filtered time series of SSTA ( $^\circ\text{C}$ ) for selected points along 45N.

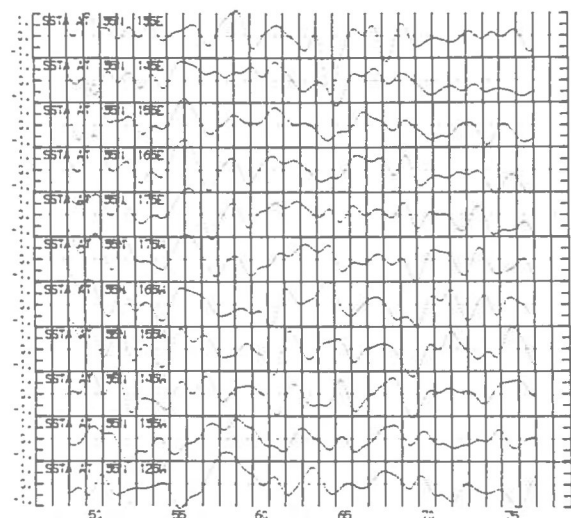


Fig. 8 Same as Fig. 7, but along 35N.

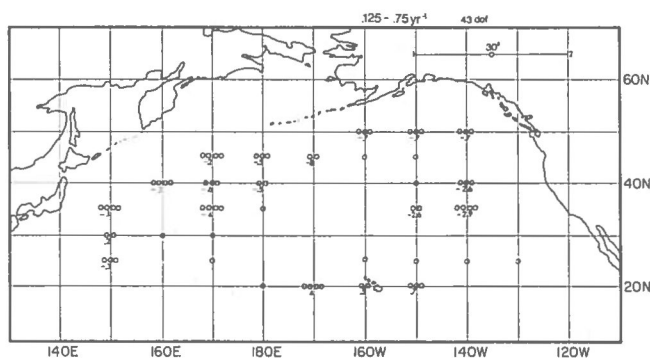


Fig. 9 Same as Fig. 5a, but for all pairs separated by 30° longitude.

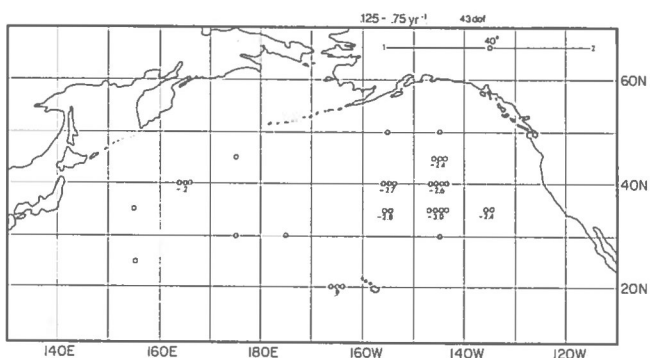


Fig. 10 Same as in Fig. 5a, but for all pairs separated by 40° longitude.

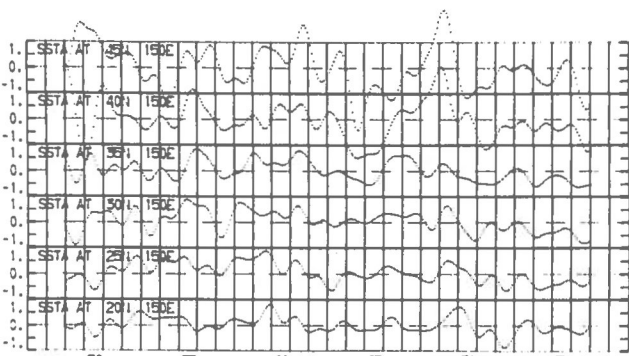


Fig. 11 Low-pass filtered time series of SSTA (°C) at all available points along 150E.

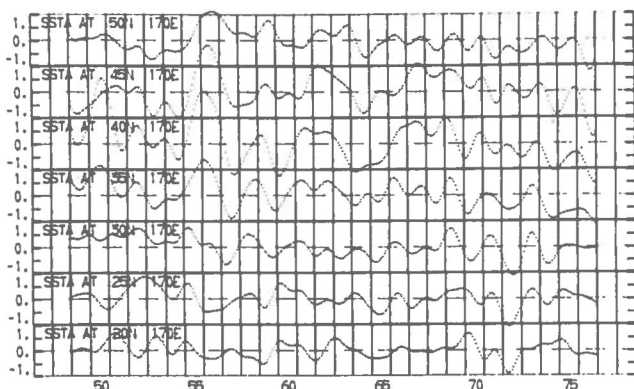


Fig. 12 Same as Fig. 11, but along 170E.

## b. Northeast (East of 165W)

In this region surface westerlies are prevalent throughout the year along 50N and 55N. Between 35N and 45N one finds a noticeable seasonal variation in the direction of predominant atmospheric surface circulation associated with the seasonal cycle in the relative strength of the Aleutian low and subtropical high pressure centers (U.S. Navy, 1956). Along the North American coast from 35N to 45N relatively persistent northerly surface flow can be found from late Spring to early Fall leading to the phenomenon of coastal upwelling.

The spatial covariance structure of SSTA in this region is marked by a noticeable decline in coherence between grid points separated by either 10° or 20° longitude along the latitude circles 35N through 45N. Zonal coherence estimates for these separations along 50N and 55N remain at the levels observed west of 165W (see Fig. 5).

Although coherence between zonally separated grid points decreases between 35N and 45N off the west coast of North America, significant coherence appears in all frequency bands between points separated by 10° latitude along and to the east of 135W (see Fig. 6). A similar relative maximum appears in the distribution (not shown) of estimates for pairs separated meridionally by 5° latitude. It seems likely that one source of meridional coherence in the vicinity of the North American coast is related to the coastal upwelling process. If the extent of the upwelling influence is judged from the region in which the roughly zonal climatological mean SST isotherms are displaced southward in summer off the west coast of the United States (Naval Oceanographic Office, 1969, pp 13-14), then the western boundary of this zone appears to be along 130W-135W in these latitudes. The plot of low-pass filtered SST at selected grid points off the North American coast shown in Fig. 13 provides some evidence that anomalies appearing over the entire region are associated with summer months. Anomalous development of the Aleutian low is likely to be related to the coherent development of winter SST anomalies along the North American coast as in 1976-77 (Namias, 1978).

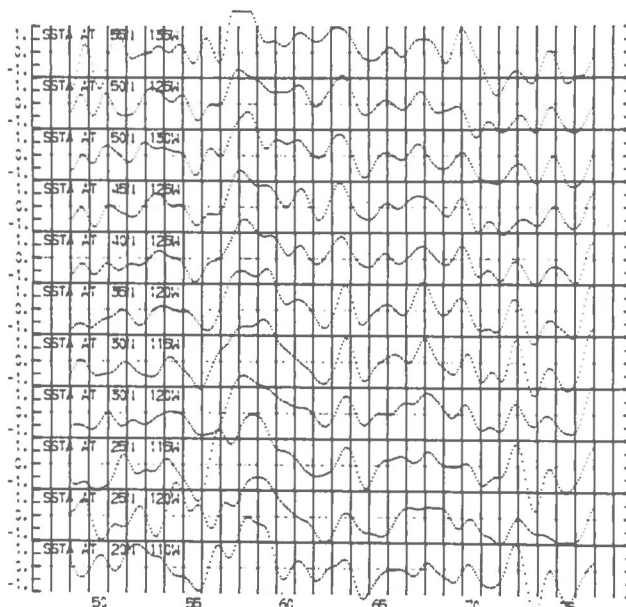


Fig. 13 Low-pass filtered time series of SSTA (°C) for selected points in the eastern Pacific.

While zonal coherence in the northeast attains a relative minimum along 35N to 45N for separations of 10° and 20° longitude, the magnitude of coherence estimates here increase significantly at separations of 30° and 40° longitude shown in Figs. 9 and 10. The small phase shifts observed for smaller separations are replaced by phase shifts of nearly  $\pi$  radians in these figures. This behavior suggests that the region from approximately 140W to 160W along 35N to 45N lies within a transition zone between regions in which SST forcing and response lead to SSTA variations of the opposite sign. The extent of these regions is more clearly defined in latter sections.

## 2. Subtropical Region (Southward from 30N)

### a. Southeast (East of 170W)

The principal climatological circulation feature of the lower troposphere in the southeastern region between 20N and 30N is the northeast trade wind system associated with the subtropical high pressure cell. The transition zone between the northeast trades and the winter westerlies occurs approximately in the vicinity of the line from 25N, 170W to 30N, 155W (Wyrski and Meyers, 1975). To the east of this line there is significant coherence on interannual time scales between grid point pairs separated by 20° longitude along 20N and 25N as seen in Fig. 5a. Figures 5b-d show much less consistent evidence of significant zonal coherence on shorter time scales. Figures 9 and 10 show that significant covariation on interannual time scales is apparent even for separations of 30° and 40° longitude along 20N. The phase estimates in these figures, as well as in Fig. 5a, indicate a slight phase lead for the eastern point of the pair over the western point.

The extension into this region of the zone of broadband coherence between points along the North American coast separated by 10° latitude is apparent in Fig. 6. Significant coherence at relatively small phase shift also appears between even widely separated grid points underlying the subtropical high (Fig. 17a). This suggests that the observed coherence primarily reflects the SST response to interannual fluctuations in either air-sea energy exchange or insolation associated with the subtropical high and the trade-wind system.

### b. Southwest (West of 170W)

In the north along 30N the southwestern region is marked climatologically by a strong seasonal variation in the direction of the prevailing surface wind (Wyrski and Meyers, 1975). In the south (around 20N) the climatological mean monthly surface flow has an easterly component throughout the annual cycle, though with a southerly component in summer replaced by a northerly component in winter. The summer southerly component becomes more pronounced in the west where the surface circulation becomes even more closely associated with the summer monsoon over South Asia (Wyrski and Meyers, 1975).

The climatological oceanic circulation features in the southwestern subtropical area are the Easterly North Equatorial current whose northern limits lie in the vicinity of 20N and the subtropical sea surface temperature front which appears (except in late summer) in the southwest between 20N, 135E and 30N, 175E.

Coherence estimates between points separated meridionally by 10° latitude in the southwest (Fig. 6) generally fall below the 90% critical value except

along 135E and 145E where estimates exceeding the 95% critical value appear in all frequency bands. The distribution of coherence estimates for pairs separated by 5° latitude (not presented) shows relatively low values west of the dateline for points along 35N and 25N paired with those along 30N. This behavior is qualitatively consistent with the observation that the vicinity of 30N marks a transition zone between mid-latitude coherence westerlies and subtropical easterlies.

Coherence estimates between points separated by 20° longitude in the southwest appear to be significantly different from zero in all the frequency bands depicted in Fig. 5 though the spatial distribution of estimates above the 95% critical value is not as uniform as in the northwestern area described above. Figure 9 reveals only one estimate of coherence on the interannual time scales at 30° longitude separation above the 95% critical value in contrast to the larger number appearing in the northwest. Thus it appears that the correlation on interannual time scales between zonally separated points is weaker in the Southwestern North Pacific than in the northwestern region.

## 3. Discussion of Regional Variations

Figure 14 combines the views of meridional and zonal coherence on interannual time scales appearing separately in Figs. 5a and 6a. In Fig. 14 the triangles represent the levels of coherence between points separated by 20° longitude shown in Fig. 5a and the circles represent the levels of coherence between points separated by 10° latitude shown in Fig. 6a. This combined view clearly suggests that the largest meridional and zonal coherence on these space scales is associated with those regions having prominent climatological features of the atmospheric and oceanic circulation. The two are not independent, of course, since the circulation of the upper ocean owes its existence largely to the wind stress distribution determined by the atmospheric wind fields overlying the ocean. The association between circulation features and large coherence lengths along the mean flows is made more intriguing by the consistency with which the phase estimates in Figs. 5a and 6a show variations

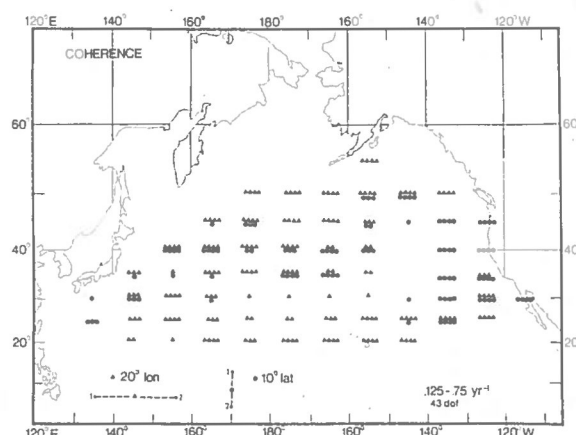


Fig. 14 Estimates of coherence in the frequency band 0.125-0.75 yr<sup>-1</sup> between points separated by 20° longitude (●) and 10° latitude (▲) taken from Figs. 5a and 6a. The numerical intervals corresponding to the number of symbols are found in Table 2. Symbols are plotted at the midpoint of the line joining the pair on the latitude-longitude grid.

on interannual time scales at the upstream point of a pair in the mean subtropical gyre having a slight phase lead over the downstream point.

As stated in the introduction to this section, the lack of quantitative, parameteric models relating cross-spectral estimates to physical processes governing SSTA evolution makes it difficult to identify which of the processes operating in given regions may be responsible for properties of the empirical estimates. The following examples illustrate the ambiguity which exists:

i. Since the east-west (zonal) coherence in the northwest occurs in a region where the predominant overlying surface winds are westerly and where there is westerly mean flow in the upper ocean, one may ask the relative importance of spatial coherence in fluctuations in these westerly currents in establishing the observed SST coherence. Since fluctuations in the wind stress distribution over the North Pacific basin will induce fluctuations in the component currents of the subarctic and subtropical gyres, it is possible that interannual variations in the westerlies will influence SST both by affecting local heat exchange and Ekman flow and through anomalous transport in oceanic current systems.

ii. The observed coherence on interannual time scales between meridionally separated points along 35N and 45N west of the dateline links interannual SST variations in the Kuroshio and Oyashio extensions. The observation that the associated phase estimates are near zero radians is qualitatively consistent with the hypothesis that large-scale heat exchange or Ekman drift anomalies associated with regional fluctuations in the westerlies are forcing the observed anomalies. It is also consistent with the hypothesis that one is seeing the influence of out-of-phase transport fluctuations in the cold Oyashio and warm Kuroshio as observed by White (1977).

Such ambiguities also obscure the conclusions of the spectral study of Reynolds (1978) which attempted to distinguish grid points in the Scripps data set where SSTA variations were plausibly forced by local heat exchange from those where nonlocal atmospheric forcing or the influence of oceanic processes may be significant. The local forcing hypothesis was judged acceptable at a grid point if, from a set of stochastic models, the spectrum of a first order Markov process linked to mixed layer response to local forcing (Frankignoul and Hasselmann, 1977) provided the best fit acceptable at the 95% confidence level to the variance spectrum estimated from the grid point SSTA series. Figure 15 is taken from Reynolds (1978) and shows the regional variation in acceptable model fit. The regions in which the two-parameter model is valid are those for which the local forcing model of Frankignoul and Hasselmann is acceptable at the 95% confidence level.

Acceptance of the first order Markov model for SSTA evaluation leads to a parameterization of cross-spectra computed here as well as the variance spectra investigated by Reynolds (1978). Since SSTA response is assumed to be a linear filter of atmospheric forcing, the coherence in the SSTA field is identical to that in the atmospheric forcing field (Koopmans, 1974). Were empirical data on the forcing fields available, it might be informative to make a comparison.

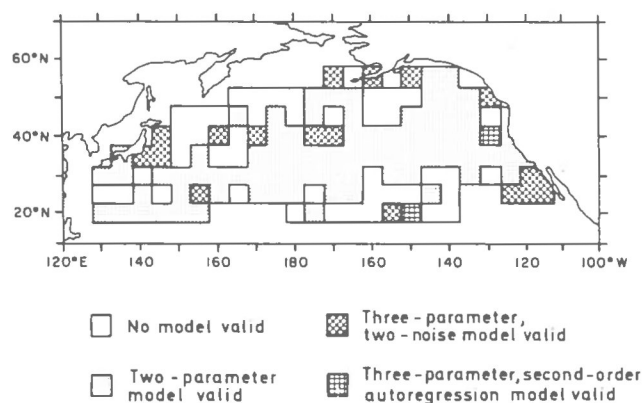


Fig. 15 Best acceptable stochastic model fit to estimated SSTA spectra for  $5^\circ \times 5^\circ$  gridded monthly data. Regions where two parameter model is valid are those where local forcing hypothesis is acceptable at the 95% confidence level. From Reynolds (1978).

With the exception of the points along 35N between 175E and 165W, along 30N from 145E to 175E, and along 135W, regions where significant meridional and/or zonal coherence in these length scales exists on interannual time scales tend to coincide with regions where the local forcing hypothesis is not acceptable. The most striking correspondence between coherence on interannual time scales and unacceptability of the two-parameter models is found in the northwest and the southeast. It is possible that both the results of Reynolds (1978) and the relatively large low-frequency coherence observed here reflect a non-local SST response to low frequency variations in the climatological centers of action in these areas.

There are, however, other reasonable hypotheses concerning the failure of the two-parameter model. The plausibility of higher frequency oceanic contributions to SSTA variance in the vicinity of the Kuroshio extension was mentioned above in connection with cross-spectral estimates. As Reynolds (1978) hints, such processes might be expected to make the three-parameter stochastic model a more acceptable choice. The present study lends some support to the hypothesis that rejection of the local forcing hypothesis is due to the contribution of oceanic processes to SSTA variability along 40N west of the dateline.

A somewhat different perspective is obtained by examining the coherence between all points lying a given distance apart along lines which are oblique to the coordinate directions in the latitude-longitude system. Figure 16 shows levels of coherence in the interannual frequency range between points separated by  $10^\circ$  latitude and  $20^\circ$  longitude along lines having slopes  $\pm 0.5$  in the latitude-longitude coordinate system. The coherence in the eastern ocean is present along these directions as well. Coherence along the lines with slope  $-0.5$  in the Northeast is generally significant only in the interannual frequency band. Coherence between points lying on lines with slope  $+0.5$  in the Southeast appears in all the broad frequency bands of Table 2. Associated phase estimates in the interannual frequency range show a tendency for variations at the northeastern point of the pair to have a small phase lead over the other.



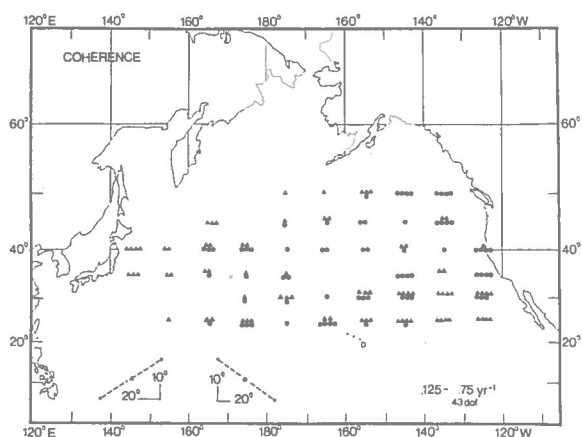


Fig. 16 Coherence in frequency band  $0.125-0.75 \text{ yr}^{-1}$  between all pairs of points separated by  $10^\circ$  latitude and  $20^\circ$  longitude along lines having slope  $\pm 0.5$  in the latitude-longitude coordinate system. Plotting of symbols and their meaning are as in Fig. 14.

The most striking new feature appearing in Fig. 16 and in estimates for the same pairs in all other broad frequency bands as well is the coherence along lines of slope  $-0.5$  north and northeast of Hawaii. The magnitude of the associated relative phase is  $2.6-3.14$  radians in all frequency bands. This suggests that the coherence 'gaps' apparent along  $30^\circ\text{N}$  and along  $145^\circ\text{W}$  may be transition zones between regions having rather different predominant forcing mechanisms. This theme is more fully elaborated in the next subsection where coherence on larger spatial scales is examined.

#### B. TRANSITION BETWEEN LOCAL-SCALE AND BASIN-SCALE COVARIANCE PROPERTIES

Although study of cross-spectral estimates between points separated by purely zonal or meridional displacements provides a reasonably concise characterization of intraregional properties, the transition to basin-scale covariance structure is most readily apparent in terms of separations along the directions defined in Fig. 16. Figure 17 presents coherence and phase estimates between pairs of data points separated along lines of slope  $+0.5$  in latitude-longitude coordinates by  $15^\circ$  latitude and  $30^\circ$  longitude. In midlatitudes the separation between pairs so displaced is approximately  $3000 \text{ km}$  which is about  $10\%$  smaller than the distance separating two points  $40^\circ$  longitude apart along  $40^\circ\text{N}$ . Comparison of Figs. 10 and 17a demonstrate that the general low level of coherence in the former is a consequence more of the zonal direction along which the separation occurs rather than of its magnitude.

Since the next section deals at some length with the spatial extent of the regions whose existence is suggested in Fig. 17, interpretive remarks at this point are limited primarily to the discussion of the frequency variation of the coherence and phase estimates involving pairs of grid points and their dependence on location in the North Pacific.

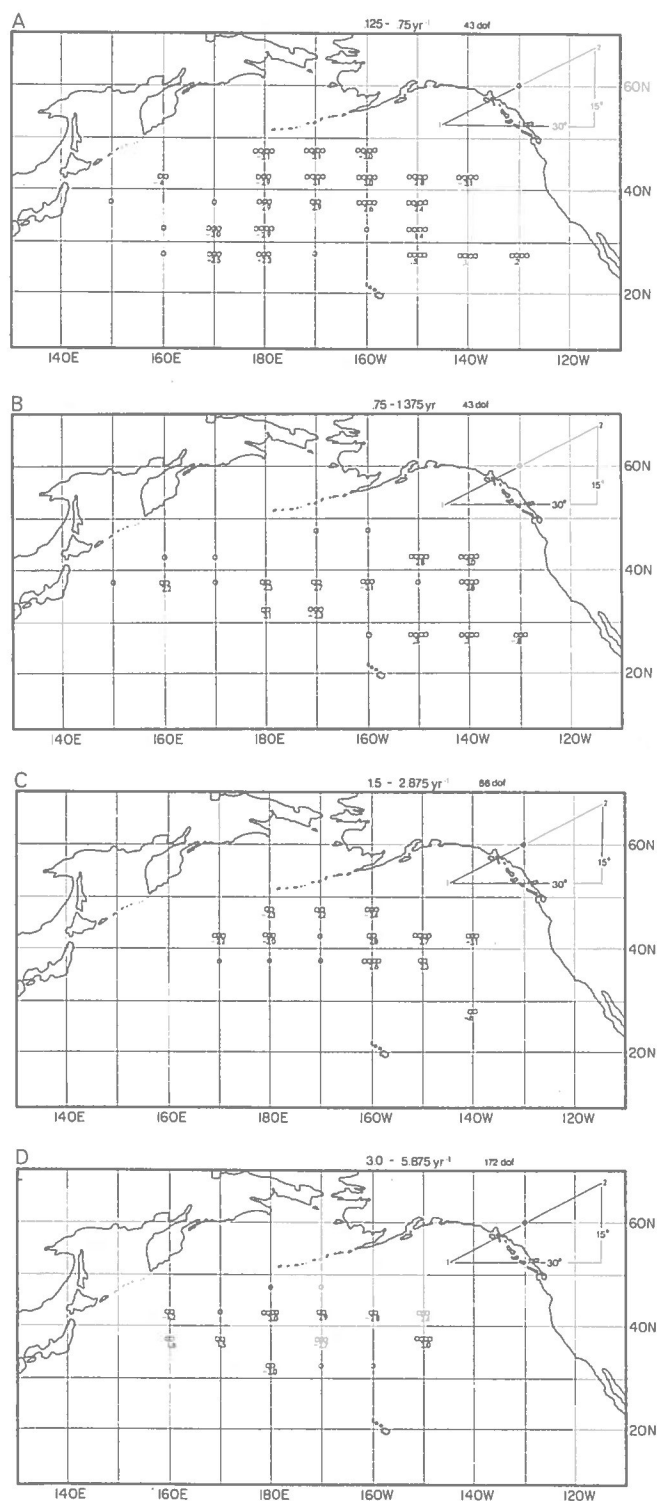


Fig. 17 Coherence and phase estimates in the frequency bands (a)  $0.125-0.75 \text{ yr}^{-1}$ , (b)  $0.75-1.375 \text{ yr}^{-1}$ , (c)  $1.5-2.875 \text{ yr}^{-1}$ , and (d)  $3.0-5.875 \text{ yr}^{-1}$  for all data pairs separated along lines of slope  $+0.5$  in latitude-longitude coordinates by  $15^\circ$  latitude and  $30^\circ$  longitude. See caption for Fig. 5 for further information.

a) Grid points east of 165W along 50N and 55W are significantly coherent with those from 165E to 155W along 35N and 40N in the interannual frequency band  $0.125\text{-}0.75\text{ yr}^{-1}$ . The high values (greater than the 99.9% critical value) of these coherence estimates allow one to conclude at the 95% confidence level that the true relative phase of these variations is approximately  $\pi \pm 0.6$  radians. This phase shift is approximately the same in all frequency bands suggesting that the mechanisms responsible for the observed large-scale coherence with phase reversal are operating, to some degree, on nearly all time scales present in the data set.

From the plots of cross-spectral estimates versus frequency in Figs. 18 and 19 for the pairs 165E, 40N with 165W, 55N and 155W, 35N with 125W, 50N, respectively, it is apparent that coherence falls off with increasing frequency. Assuming that the atmospheric contribution to the forcing function responsible for the observed coherence is relatively independent of frequency over the range considered here as argued by Frankignoul and Hasselmann (1977), the decrease of coherence with increasing frequency could reflect a lowered signal-to-noise ratio due to the weaker SST response to higher frequency forcing suggested by the arguments of these authors. Signal amplitude on time scales shorter than one year may also be reduced by seasonal variations in spatial structure of the forcing fields. On the other hand, high frequency noise may be enhanced by processes forcing SSTA variations which are incoherent on the interregional length scales considered in Fig. 17.

Some insight into high frequency noise and its detection by cross-spectral means can be obtained by noting first that the high level of coherence extends

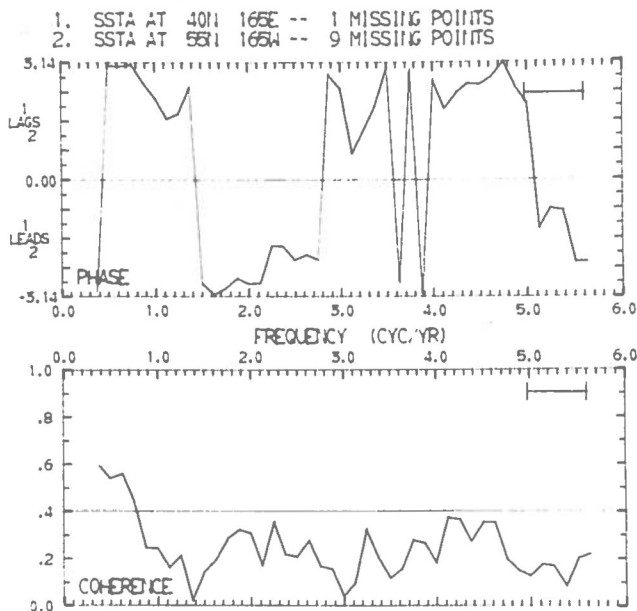


Fig. 18 Coherence and phase estimates between SSTA at 165E, 40N and 165W, 55N. Estimates obtained by 5-point frequency average of ensemble averaged estimates for 4 blocks of 96 months. Resolution bandwidth is shown in upper right of plots. Horizontal line on coherence plot indicates critical value for rejecting zero coherence null hypothesis at 95% confidence level.

to higher frequencies for the eastern pair (Fig. 19) than for the western pair (Fig. 18). The variance spectrum for data at 165E, 40N presented in Fig. 20 shows a marked flattening at slightly below  $1\text{ yr}^{-1}$  which is roughly where the low frequency coherence in Fig. 18 falls to levels below the 95% critical value. Reynolds (1978) (see Fig. 5) argues that the better fit to this spectrum provided by the three parameter (two noise) model suggests that processes other than local heat exchange significantly affect SSTA here. Recalling the cross-spectral estimates (Figs. 18-19) it can then be suggested that this additional force has a smaller correlation length scale than that which

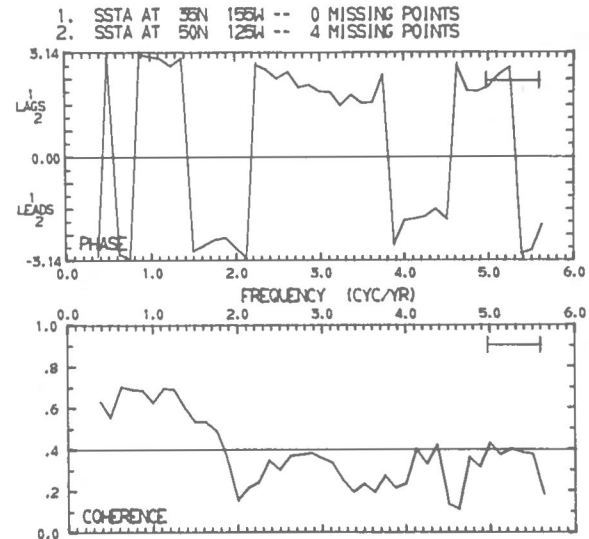


Fig. 19 As in Fig. 18, but between 155W, 35N and 125W, 50N.

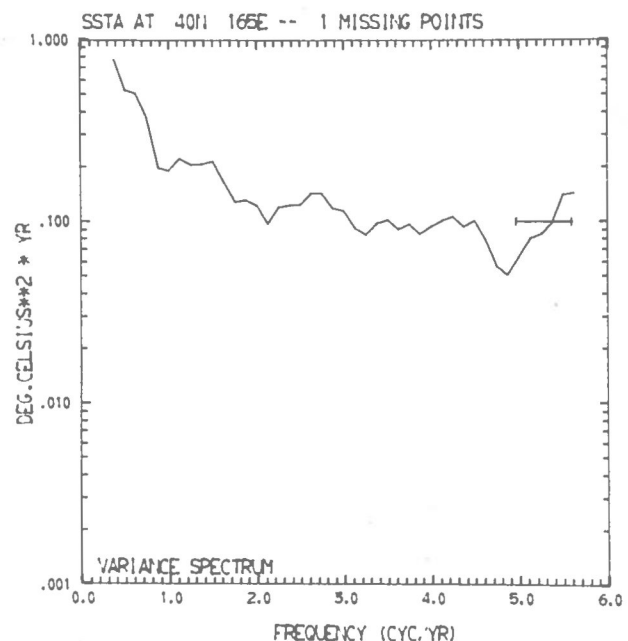


Fig. 20 Variance spectrum of SSTA at 165E 40N computed by applying 5 point frequency averaging to ensemble averaged estimates from 4 blocks of 8 years.

is predominant in the lower frequencies. Oceanic processes associated with the eastward extensions of the major gyres into the vicinity of 165E 40N are likely candidates for this nonlocal forcing of SSTA. This example shows that a combination of auto- and cross-spectral analyses of the SSTA field may yield sharper insights into the origins of the spatial and temporal structure of the field than when taken alone.

b) In the central and southwestern North Pacific, Fig. 17a reveals apparent coherence between the region between 155E and 165E along 20N and 25N and that between 175W and 165W along 35N and 40N. The relative phase of variations at these points on inter-annual time scales is somewhat less than  $\pi$  radians with phase shifts smaller between pairs from 20N and 35N than from 25N and 40N. Thus these estimates suggest a low frequency association between SST variations in a portion of the western region influenced by subtropical easterlies and those subjected to mid-latitude westerlies.

c) The coherence noted in Fig. 17a between pairs along 20N east of 165W and along 35N east of 135W, the latter having a slight phase lead over the former, has been recognized in the previous discussion of the southeastern region. The rather uniform increase in phase associated with the coherence estimates north of the southeastern region along 150W is intriguing and may contain potentially useful information concerning the transition from one region to another.

Figure 21 presents coherence and phase estimates between data pairs separated along lines of slope -0.5 in latitude-longitude coordinates by 15° latitude and 30° longitude. Most estimates in Fig. 21a which

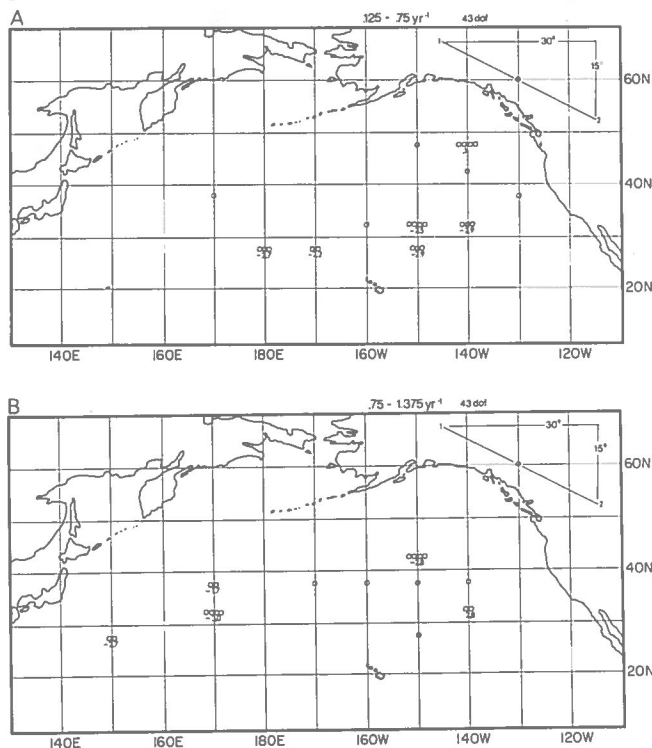


Fig. 21 As in Fig. 17, except separations are along lines of slope -0.5.

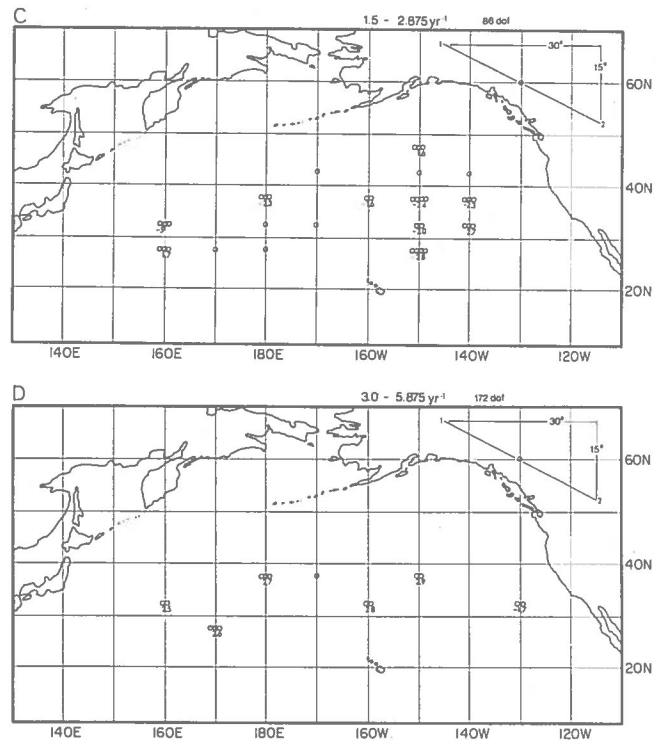


Fig. 21 (Continued)

exceed the 95% critical value indicate a relationship between variations in the southeast region and east-central regions in which the phase lead of variations in the latter over those in the former is nearly  $\pi$  radians in the interannual frequency band. Figures 21b-d show little evidence of significant patterns of covariance in terms of coherence although the phase estimates in all frequency bands tend to be of the same magnitude as those in Fig. 21a.

Taken together the results presented in Figs. 10, 17a, and 21a strongly suggest a significant tendency for interannual SST variations in the East-Central North Pacific to be out-of-phase with interannual SST variations along the North American coast from the Gulf of Alaska to the subtropical Pacific east of the Hawaiian Islands. This tendency appears to be strongest on all time scales north of 35N. Figure 17a further suggests an association on interannual time scales between SST variations in the Southwestern North Pacific and the Central North Pacific across the region near 30N which coincides with the climatological transition zone between midlatitude westerlies and subtropical easterlies. A more systematic delineation of these apparent basin-scale relations is presented in the next section.

#### IV. BASIN SCALE COVARIANCE STRUCTURE

This section presents a more concise and intelligible view of the basin-scale linear associations in the SST field which emerged above in the systematic study of grid point pairs. Previous attempts to characterize large-scale interrelationships in variations in the SST field have often used empirical orthogonal function (EOF) patterns as the basis for discussion

(Davis, 1976, 1978; Weare et al., 1976; Weare, 1977; Barnett and Preisendorfer, 1978). Although the utility of truncated EOF representations of data fields in statistical prediction has long been recognized in the atmospheric sciences (e.g. Lorenz, 1956), slower progress has been made toward the goal of setting forth criteria for recognizing statistically significant features of the EOF patterns (Craddock, 1973; Preisendorfer and Barnett, 1977).

An alternate method for reducing information in a data field to more manageable dimensions is to average the data over larger length scales than those in which it is reported. Large-scale interregional relationships can be concisely presented if sufficient insight is available to identify the regions. The necessary insight may come from knowledge of the dominant physical processes differentiating the regions. When - as in the case of SST - the complexity of forcing and response makes a priori identification of dominant mechanisms difficult, statistical tests of association such as those described above may serve as a guide to identifying regions. Regions and regional relations suggested by statistical analyses must, of course, be weighed against available dynamical insight with the goal of testing and improving both. In the case of North Pacific SST, comparisons can be made with EOF patterns obtained by Davis (1976) and Weare et al. (1976). The present study should be viewed as an alternative approach providing a different view of the statistical and, perhaps, physical significance of structures appearing in EOF patterns.

In this report only the problem of defining regions by their covariation on interannual time scales is addressed. This restriction is introduced, first, because understanding of the interrelationship between ocean and atmosphere on these time scales is

the principal goal of this research program and, second, because it is on these time scales that the analysis described above suggests the large-scale patterns of SSTA covariation to be strongest. It is worth recalling here that seasonal variations in the fields forcing SSTA variation may tend to obscure shorter time scale regional relations and that seasonal stratification of the data may be required to expose the important dynamical relations even on interannual time scales.

The sensitivity of boundaries to the significance level chosen as an indicator of coherence may conceivably introduce unacceptable arbitrariness in boundaries. Fortunately the regions identified here are, with one arguable exception, separated by zones having rather distinct coherence and phase gradients. Boundary identifications are therefore relatively insensitive to the choice of critical value for rejecting the zero coherence null hypothesis.

The structure of basin scale SSTA covariation on the interannual time scales accessible in the records employed here is depicted in Figs. 22-25. Each figure presents contours representing the phase and coherence estimates between SSTA at grid points shown in Fig. 1 and the time series of SSTA averaged over the region outlined in the figure. The contours were obtained by visual interpolation of the spatial array of coherence and phase estimates for the interannual frequency band,  $0.125-0.75 \text{ yr}^{-1}$ . Since confidence limits on phase estimates depend on the associated coherence it is not possible to present them succinctly on the figures. It may be useful to note that if the coherence estimate is below the critical value at a given confidence level then the confidence limits on phase at the same level will include the entire interval

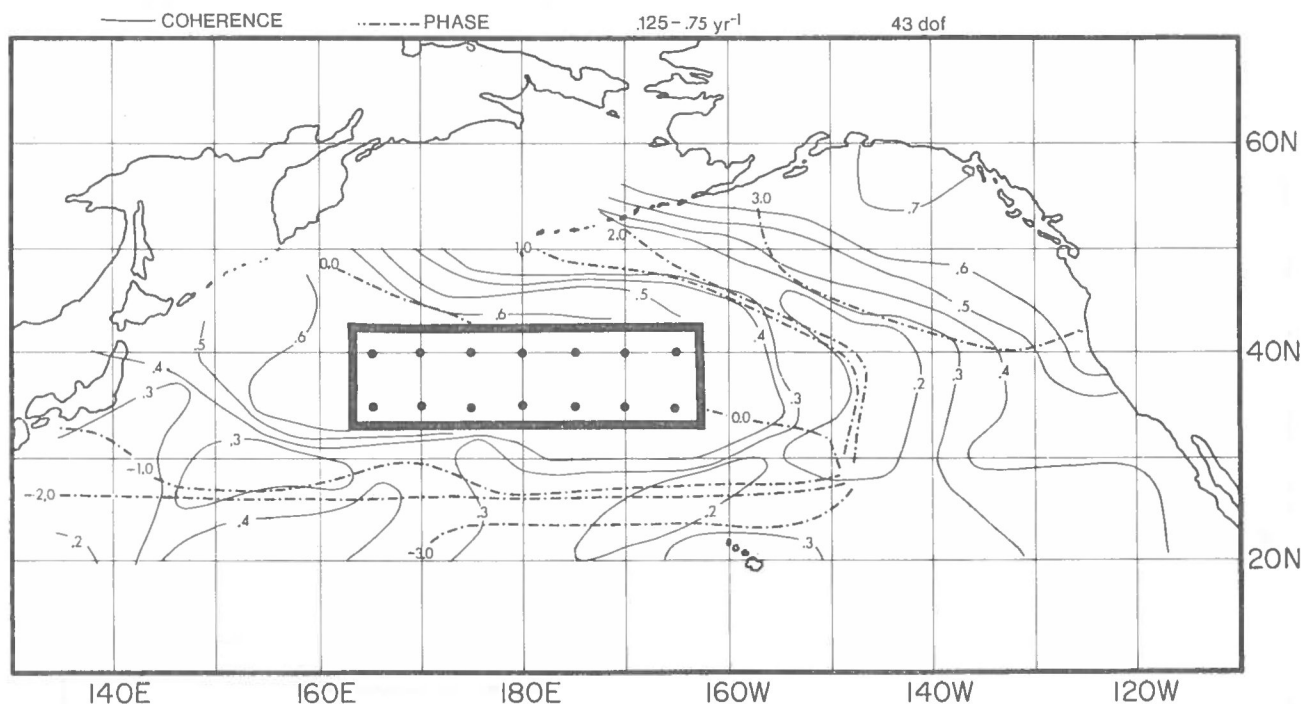


Fig. 22 Visually contoured coherence and phase estimates in frequency band  $0.125-0.75 \text{ yr}^{-1}$  between SSTA in mid-North Pacific area (sometimes denoted MIDPAC) and other grid points. Positive value of phase estimate indicates that the area averaged SSTA leads grid point.



$[-\pi, \pi]$ . In short, at this confidence level nothing can be concluded about the phase. Low-pass filtered time series of the SSTA variations for the areas defined in Figs. 22-25 are plotted in Fig. 26. The following discussion focuses first on the Central and Eastern North Pacific after which the relationship between the southwestern area and the rest of the basin is considered. The final subsection discusses

some relationships between the North Pacific regions and two data sets known to reflect important inter-annual variations in the atmosphere-ocean system in the tropical Pacific.

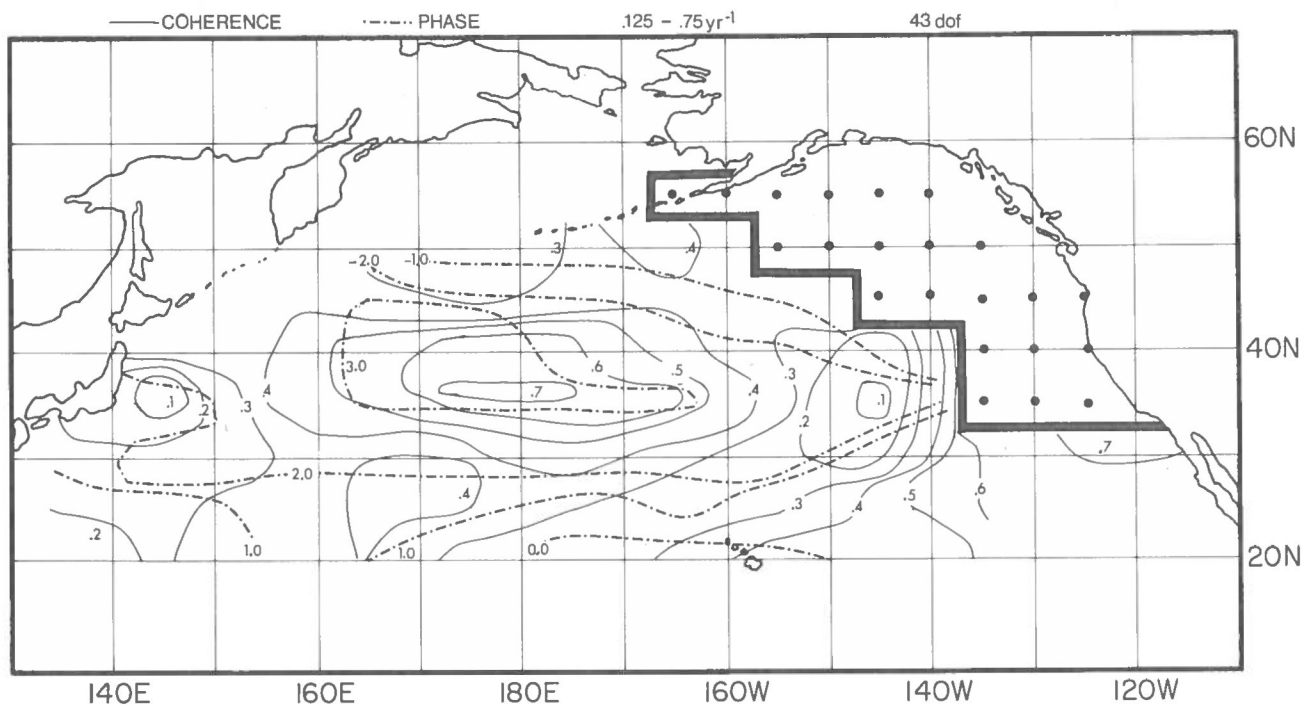


Fig. 23 Same as Fig. 22, but for northeastern region (NEPAC) of North Pacific.

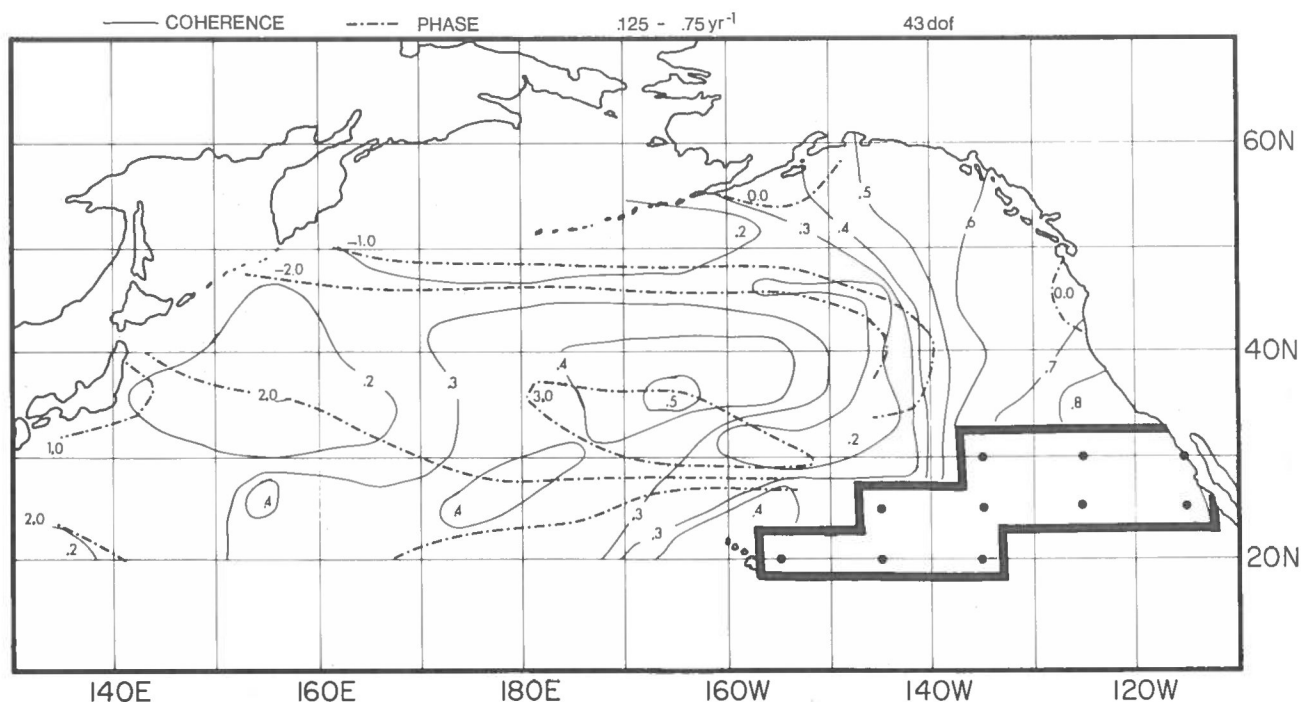


Fig. 24 Same as Fig. 22, but for southeastern region (SEPAC) of North Pacific.

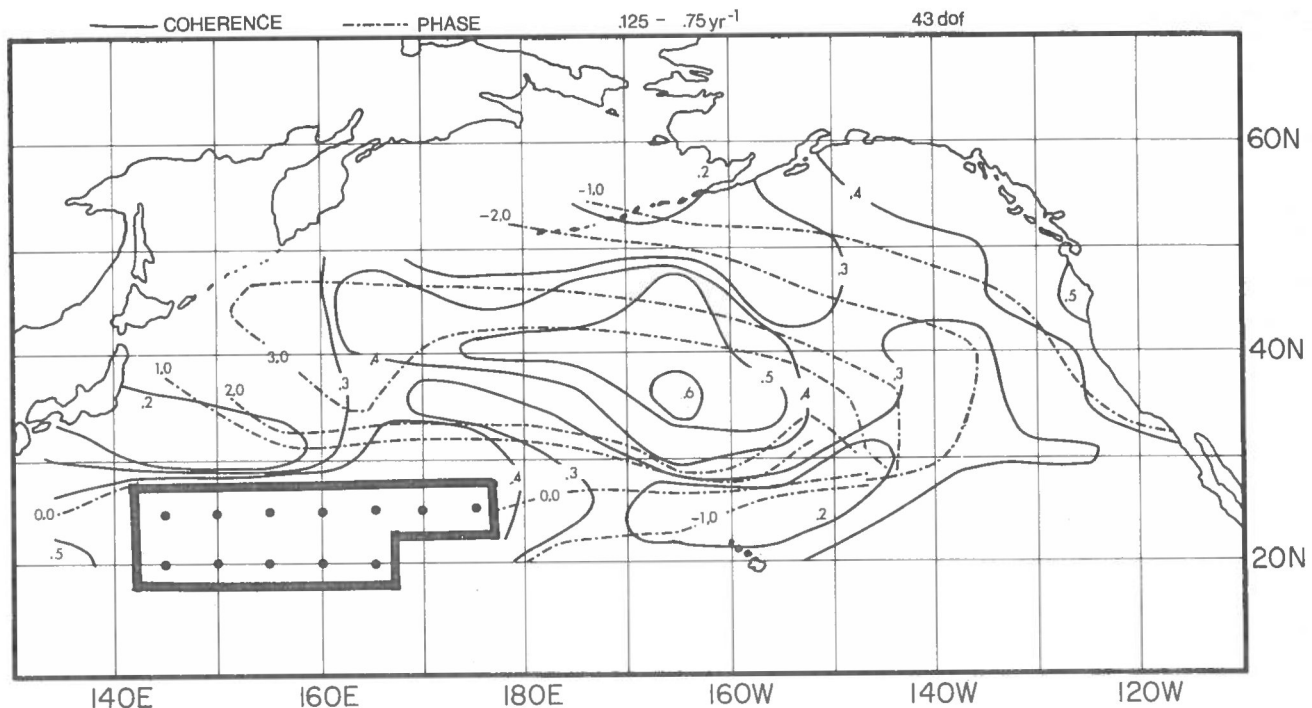


Fig. 25 Same as Fig. 22, but for southwestern region (SWPAC) of North Pacific.

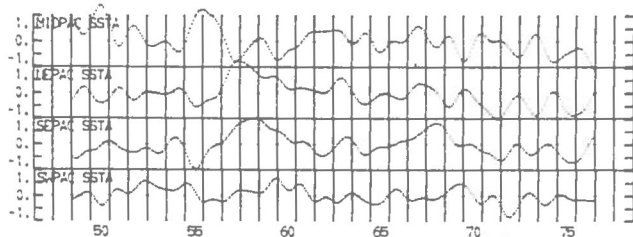


Fig. 26 Low-pass filtered time series of SSTA ( $^{\circ}\text{C}$ ) for North Pacific regions defined in Figs. 22-25. Cut off frequency is  $0.78 \text{ yr}^{-1}$ .

#### A. THE EASTERN NORTH PACIFIC SEESAW

The areas defined in Figs. 22 and 23 were chosen from a screening of the cross-spectral estimates between data point pairs. The estimates discussed in the last section and others which are not presented here provide a rough indication of the regional boundaries. The existence of coherence on interannual time scales between most pairs of data points within each of these regions is strongly supported by Fig. 5a for the Central Pacific region in Fig. 22 and by Figs. 6a and 16 for the Northeast Pacific region defined in Fig. 23.

Figures 22 and 23 show distinctly that variations on interannual time scales in the Central North Pacific region are coherent and nearly  $\pi$  radians out of phase over the entire data set within the boundaries of the Northeastern North Pacific region and vice versa. The transition zone between these two regions is marked by a decrease in coherence and a systematic increase in relative phase toward the northeast. The broadband character of the relationship between these regions can be seen from the cross-spectral estimates

computed from the time series of area averaged SSTA for the central and northeastern regions defined in Figs. 22 and 23. These estimates are presented in Fig. 27. Although the estimated coherence is largest on interannual time scales, it appears to exist in the vicinity of the 95% critical value for most frequencies. The corresponding phase estimates are rather uniformly near  $\pm\pi$  radians.

The southern boundary of the northeastern region in Fig. 23 was chosen along  $35^{\circ}\text{N}$  in order to reflect the weakening of the association between variations in the Central Pacific and those in the coastal zone apparent in Fig. 22. It is clear from Fig. 23 that the northeastern region is significantly correlated with points in the Southeastern North Pacific. Furthermore from the figures described in Section III, it is clear that within the southeastern region significant coherence at relatively small phase shift is found on interannual time scales. These figures also indicate that SSTA variations in the southeast are coherent with those in the Eastern Central Pacific but phase shifted by approximately  $\pi$  radians. These observations motivate the definition of the Southeastern North Pacific region in Fig. 24.

The broadband nature of the relationship is evident from the cross-spectra of the time series of these area averages shown in Fig. 28. The clear implication is that some of the processes causing SST variation in the Eastern North Pacific off the North American coast operate more or less coherently and simultaneously from the Gulf of Alaska to the subtropical Pacific east of Hawaii on all time scales from a few months to several years.

Relatively high coherence is apparent in Fig. 24 between the southeastern region and grid points in the Central North Pacific. The coherence maximum in Fig. 24 is shifted eastward to  $165^{\circ}\text{W}$  as opposed to  $180^{\circ}\text{W}$  as shown in Fig. 23. Furthermore, Fig. 24 shows that the

coherence between the southeastern area and the portion of the central area west of the dateline is nowhere greater than the 90% critical value.

The coherence estimates for variations in the southeastern and central Pacific areas shown in Fig. 29 are generally below the 95% critical value though the value for the lowest frequency band is an exception. Although these values are low, the associated phase estimates tend to be predominately near  $\pm\pi$  radians. The low coherence estimates between the central and the southeastern region no doubt reflect the relative low coherence apparent in Fig. 24 between the latter and grid points in the western half of the mid-Pacific region.

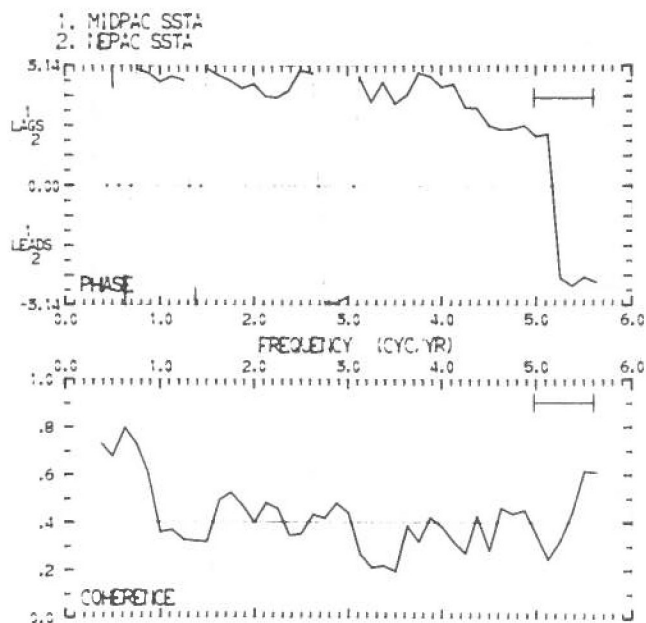


Fig. 27 Coherence and phase estimates using time series of SSTA averaged over areas defined in Figs. 22 and 23. For more information see caption of Fig. 18.

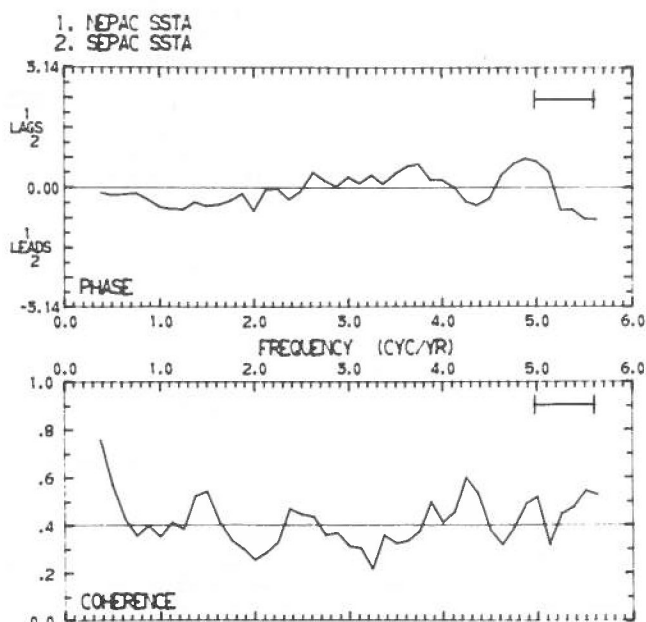


Fig. 28 As in Fig. 27, but for areas defined in Figs. 23 and 24.

The phase relations among the three regions identified in Figs. 22-24 are consistent with those of the principal empirical eigenvector of North Pacific monthly mean SST anomalies computed by Davis (1976) and Weare et al. (1976). The first two EOF patterns reported by Davis (1976) are reproduced here in Fig. 30. Comparison of the principal eigenvector pattern  $T_1$  in Fig. 30 with Figs. 22-25 shows the contours of amplitude in the former correspond closely to those of coherence in the latter.

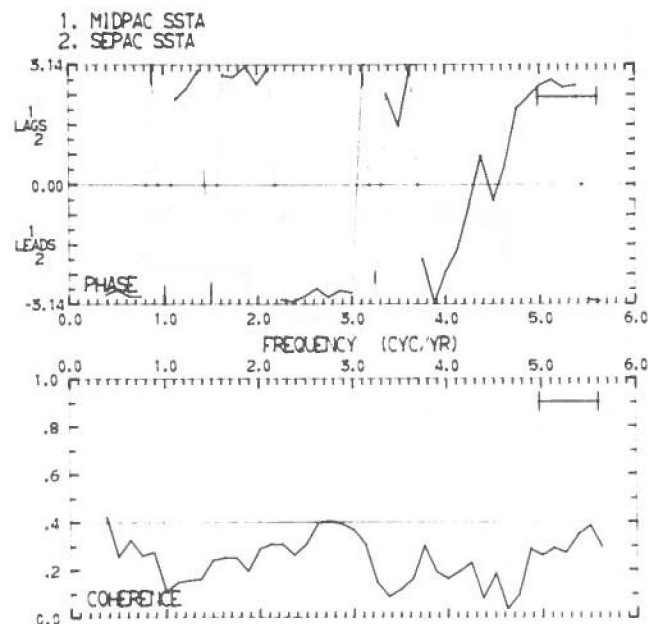


Fig. 29 As in Fig. 27, but for areas defined in Figs. 22 and 24.

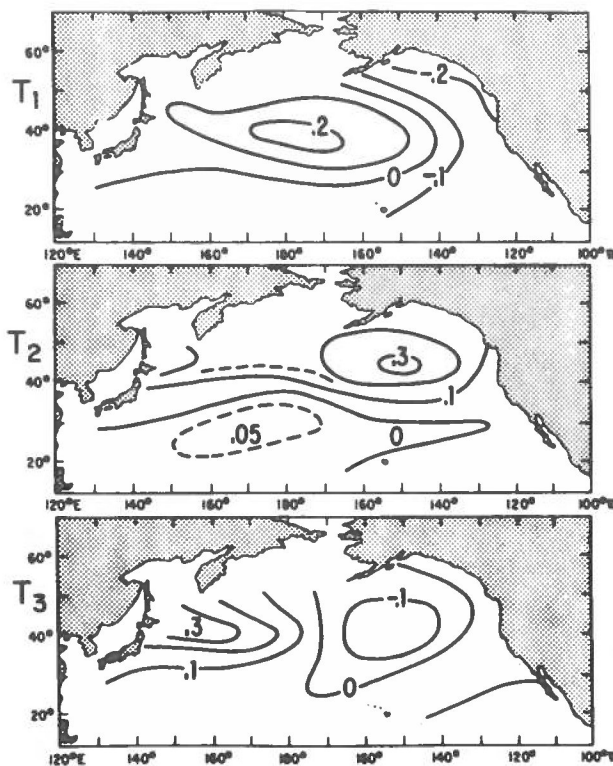


Fig. 30 Principal empirical orthogonal functions of sea-surface temperature anomaly. From Davis (1976).

A potentially useful interpretation of this relationship is obtained by viewing the spatial structure of temporal SSTA variations as the sum of a "signal" whose spatial distribution of variations at any given time is determined by  $T_1$  with "noise" having relatively uniform variance over the North Pacific basin. The noise would be relatively more important in regions of small signal amplitude yielding lower coherence estimates, hence the distribution of coherence estimates would resemble that of signal amplitude. This suggests that significant insight into both SST forcing and response fields may come from understanding the physical basis for the principal EOF pattern shown in Fig. 30.

Among the most likely origins for the signal in the  $T_1$  pattern are the atmospheric fluctuations represented by the principal empirical eigenvector,  $P_1$ , of the sea-level pressure anomaly field computed by Davis (1976) and reproduced here in Fig. 31. Davis has computed the cross-correlation function between  $T_1$  and  $P_1$  finding a significant peak with  $P_1$  leading  $T_1$  by 1 month. Certainly the indicated anomalous geostrophic flow could be associated with anomalous heat transports and anomalous wind driven surface currents which may plausibly yield out-of-phase SSTA variations in the Northeastern and Central North Pacific.

A suggestion for the connection of the southeastern region to the seesaw between the Central and Northeastern Pacific regions appears in the investigation of atmospheric teleconnections associated with El Niño by Namias (1976). He observes a weakening of the subtropical high east of Hawaii and a deepening of the Aleutian low in those winters in which the East Equatorial Pacific is anomalously warm (El Niño). This relationship between the Aleutian low and the East Pacific subtropical high is apparent in  $P_1$  (Fig. 31). If reduced trade winds are associated with a weakened subtropical high then reduced heat and water vapor transport from ocean to atmosphere and reduced coastal upwelling might lead to warm SST anomalies in the southeast roughly simultaneous with warm SST in the northeast due to the deepened Aleutian low. Increased cloud cover hence decreased isolation tending to lower SST might, however, accompany the weakening subtropical high.

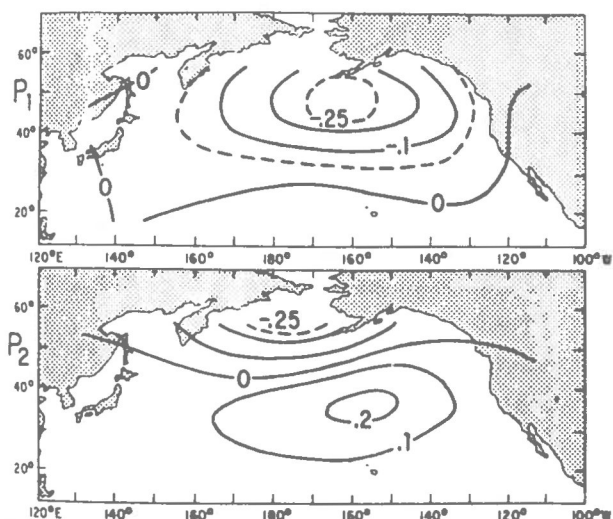


Fig. 31 As in Fig. 38, but for sea level pressure anomaly. From Davis (1976).

## B. RELATIONS WITH THE SOUTHWESTERN NORTH PACIFIC

The rather clear distinction appearing between the central and eastern regions is not characteristic of the covariance structure revealed west of the date line. Examination of the Southwestern North Pacific area in Figs. 22 and 23 reveals that in each there are points, generally south of 30N and between 145E and 175E, for which coherence estimates with the regional averages are significant at the 95% confidence level. In each of these figures a band of somewhat lower coherence appears along 30N between the Central North Pacific region and these southwestern points. In Fig. 22 it is apparent that this band coincides with the zone in which the phases of the grid point variations relative to those of the Central North Pacific area average change by nearly  $\pi$  radians.

Further evidence is provided by the cross-spectral estimates for data pairs displaced along southwest-northeast lines presented in Fig. 17a. On interannual time scales, variations at data points between 155E and 165E along 20N and 25N are significantly coherent with those at 175W and 165W along 35N and 40N. The associated phase estimates lie between -2.3 and -3.0 radians. The levels of coherence are not sufficiently high so as to allow the phase to be confidently distinguished from  $\pi$  radians. These observations together with the fact that the subtropical oceanic front existing in this region exhibits detectable secular variability apparently related to that of other North Pacific circulation phenomena (White et al., 1978) motivate the further consideration of the southwestern region as a significant basin feature.

Figure 25 presents the relationship between variations averaged over one plausible definition of a southwestern region and grid points over the remainder of the North Pacific. Studies using subsets of points entering the region shown in Fig. 25 suggest that the uncertainty in the southwestern area boundary is not so large as to affect the general observations made here concerning its relation to the remainder of the North Pacific SSTA field. The Central and Eastern North Pacific regions stand out with relatively high values of coherence on interannual time scales. The phase estimates suggest that the southwestern region is approximately in phase with the northeastern area while having a phase shift of  $\pi$  radians relative to variations in the Central North Pacific. As in the study of the southeastern region in Fig. 24, the Central Pacific area of maximum coherence with the southwestern region occurs at 165W 35N. Relative to this point, however, the southwestern region has, an estimated phase lead of 2.3 radians which is significantly different (at the 95% confidence level) from its phase lead over 165W 45N (-2.9 radians) where the coherence also exceeds the 99.9% critical value. The implied phase shift between these points along 165W is apparent in the direct cross-spectral analysis of their relationship (see Fig. 6a).

Another apparent feature of the relationship presented in Fig. 25 is the relatively high coherence estimated along 45N in the Central Pacific and the relatively low coherence estimated west of the date line along 35N. This reverses the situation in the West Central Pacific apparent in Fig. 23. Thus, the northeastern area appears to be coherent with and approximately  $\pi$  radians out of phase with the West Central Pacific along 35N and 40N whereas the southwestern area defined in Fig. 24 is coherent with and

approximately  $\pi$  radians out of phase with the west central Pacific along 40N and 45N. Since the climatological position of the subarctic convergence separating the subarctic and subtropical gyres is along 40N this difference is worth more careful consideration than its statistical basis alone might suggest.

The relationship shown in Fig. 25 between the southwestern area and points in the northeastern and southeastern regions is largely what may be anticipated from Figs. 23 and 24. The coherence estimates involving points along the west coast of North America are generally above the 95% or 99% critical value. The associated phase estimates decrease from about -0.6 radian in the Gulf of Alaska to about -1.4 radians at 115W 25N. The magnitude of the coherence estimates is not sufficiently large so that the 95% confidence limits placed on the phase estimates exclude zero radians. Nonetheless, the uniformity of the phase lag of the southwestern area over these points along the North American coast suggests that, in the interannual frequency band, the southwest may truly exhibit a phase lag of  $0.25\pi$  -  $0.5\pi$  radian over points in the Northeastern and Southeastern North Pacific regions.

Cross-spectra of the time series of area-averaged SSTA over the southwestern region with the regions defined in Figs. 22-25 are shown in Figs. 32-34. In Fig. 32 it is clear that the northeastern region leads the southwestern region by approximately  $0.25\pi$  radians over a broad range of time scales including the interannual time scales for which the coherence estimates are significant at the 95% confidence level. The phase lead of the southeastern area over the southwest (Fig. 33) appears to be more nearly  $0.5\pi$  radians though the magnitude of the coherence estimates on interannual time scales is lower than those in Fig. 32. The phase shift between the mid-North Pacific region and the southwest (Fig. 34) is approximately  $\pi$  radians in the interannual frequency band.

Unlike the existence of the regions identified in Figs. 22-24, that of the southwestern region in Fig.

25 is only weakly supported by the  $T_1$  eigenvector pattern of Davis (1976) shown here in Fig. 30. Both  $T_1$  and the principal nonseasonal eigenvector (NS1) of Weare et al. (1976) suggest that variations in the southwestern region are in phase with those in the East while being out-of-phase with variations in the Central North Pacific. The time lagged association between the southwestern and other regions which is suggested by the phase estimates presented here would be reflected in the small amplitude of the southwestern region in  $T_1$ .

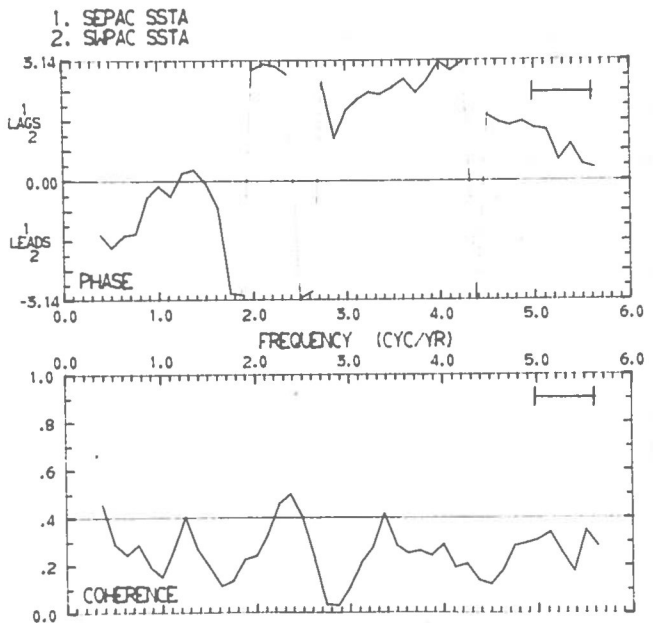


Fig. 33 As in Fig. 27, but for areas defined in Figs. 24 and 25.

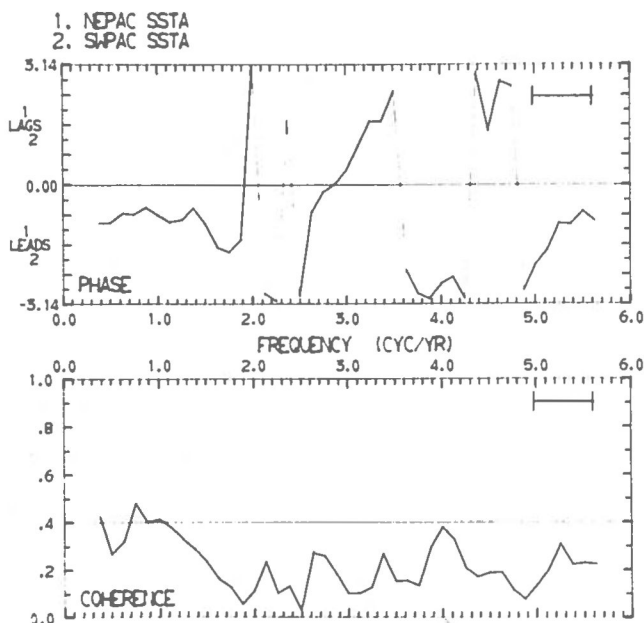


Fig. 32 As in Fig. 27, but for areas defined in Figs. 23 and 25.

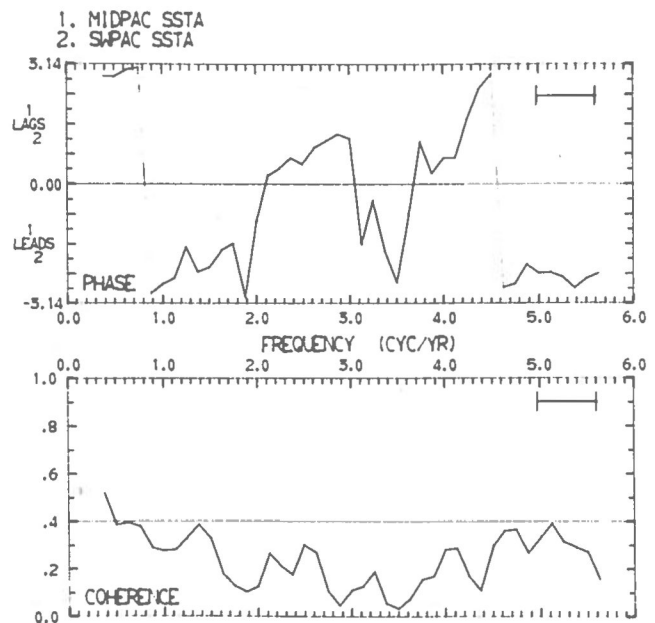


Fig. 34 As in Fig. 27, but for areas defined in Figs. 22 and 25.



Identification of physical mechanisms potentially responsible for the apparent linear association of SSTA variations in the southwest with those in the other areas would support the physical reality of these empirical associations. Since both the southwestern and the southeastern regions are overlain by the subtropical easterly circulation system and coincide roughly with the southward and westward branches of the North Pacific subtropical gyre, it might be anticipated that their relationship would be the most clearly defined and the most easily explained. It is apparent, however, from Fig. 25 and Figs. 32-34 that the southwestern region is more strongly associated with the Central and Northwestern North Pacific regions than with the southeastern region.

### C. THE TROPICAL CONNECTION

Important insight into the nature and origin of the associations described above can be obtained by considering the relationships with various tropical Pacific atmospheric and oceanic parameters related to both the Southern Oscillation and the El Niño phenomenon. This subsection describes some preliminary results of this analysis which provide striking qualitative support for the interrelationship between tropical and midlatitude circulation systems suggested by Bjerknes (1966, 1969).

In Figs. 35 and 36 cross-spectral estimates are presented between SSTA in the Northeastern and Central North Pacific regions (Figs. 22 and 23) and the time series of SST anomalies at Puerto Chicama, Peru (7S, 79W). Julian and Chervin (1978) show there to be very significant coherence between the Southern Oscillation index and standardized Puerto Chicama SST in a band peaked at 2.8 years. In the present study, Puerto Chicama SST anomalies are defined relative to the mean monthly means of the period of overlap with the North

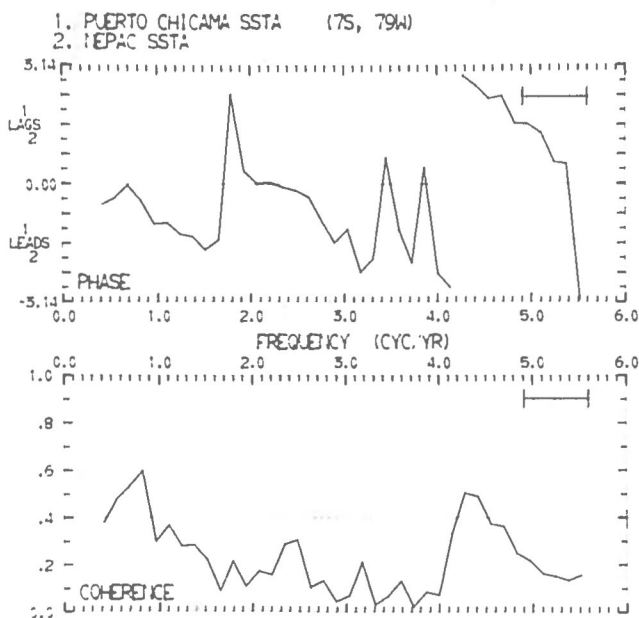


Fig. 35 Coherence and phase estimates between Puerto Chicama SSTA departures from mean monthly means in the period 1947-1976 and SSTA averaged over the Northeastern North Pacific region defined in Fig. 23. Estimates obtained by five-point frequency average of ensemble averaged estimates for four blocks of 90 months.

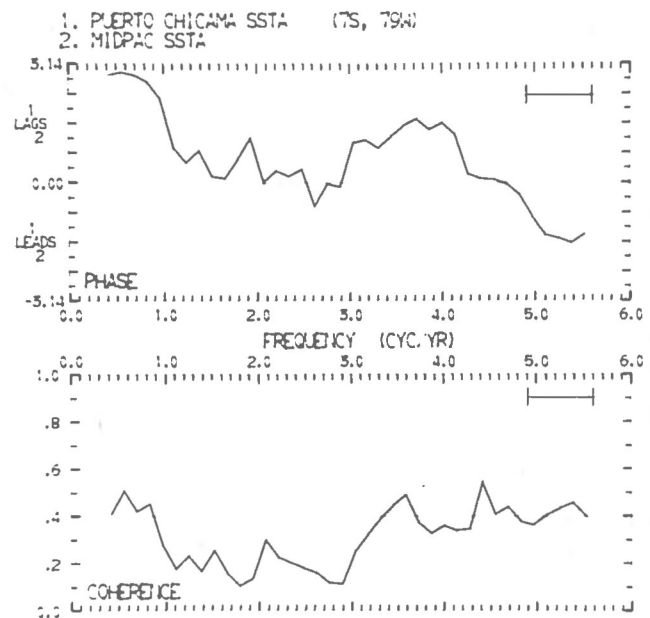


Fig. 36 As in Fig. 35, but for Central North Pacific area defined in Fig. 22.

Pacific data (1947-1976). In both Figs. 35 and 36 there is clearly significant coherence on interannual time scales. Associated phase estimates indicate a slight phase lead for Puerto Chicama SST over the Northeastern region, whereas there is nearly a phase shift of  $\pi$  radians between Puerto Chicama and the Central Pacific region. The phase relationships between these regions are those implied by the principal nonseasonal EOF of Pacific SST found by Weare et al. (1976). The fact that the regions of maximum amplitude in this EOF are seen here to be significantly coherent on interannual time scales supports the claim by Weare et al. (1976) that the El Niño phenomenon is a feature extending well into the North Pacific basin.

The observed association between midlatitude SST and eastern equatorial Pacific SST seems, on the basis of available evidence, most naturally interpreted in terms of the mechanism first described by Bjerknes (1966, 1969). The appearance in the Northern Hemisphere winter of abnormally warm water in the eastern equatorial Pacific accelerates the Hadley circulation in this longitude sector which, Bjerknes observed, could increase the angular momentum flux to the midlatitude westerlies resulting in their intensification. Namias (1976) has observed that the Aleutian low deepens and shifts southward of its climatological position during El Niño winters. If it is accepted that the principal EOF,  $P_1$ , of sea-level pressure anomaly (Fig. 31) reflects such variations in the westerlies then the significant correlation between  $P_1$  and  $T_1$  (Fig. 30) with the former leading by one month would suggest that  $T_1$  may contain the SST response to midlatitude atmospheric circulation anomalies arising through the Bjerknes mechanism. The cross-spectral analysis described above provides direct empirical evidence of the Southern Oscillation-El Niño signal in midlatitude North Pacific SST variations.

Further perspective on the association between the equatorial Pacific and midlatitudes is seen by repeating the above analysis with the Line Islands

precipitation index. The cross-spectral estimates shown in Fig. 37 show a significant association between Puerto Chicama SST and Line Islands precipitation index in a broadband apparently peaked at a period of two years. The phase estimates show positive precipitation anomalies slightly lagging warm SST anomalies at Puerto Chicama. It is therefore plausible to view the low frequency Line Islands precipitation variations as, in large part, a response to changes in the eastern equatorial Pacific sea surface temperature associated with the Southern Oscillation. From Figs. 38 and 39 it is clear that a significant association exists on interannual time scales between variations in the index and the North Pacific SST averaged over the regions in Figs. 22 and 23. Note that the phase estimates are shifted by roughly the phase shift between the precipitation index and Puerto Chicama SST shown in Fig. 37. These results further support the claim of nearly instantaneous telecommunication of tropical atmospheric and oceanic anomalies related to the Southern Oscillation and El Niño to midlatitude North Pacific SST.

The mechanisms responsible for the apparent associations involving the subtropical regions defined in Figs. 24 and 25 are to a lesser extent illuminated by knowledge of interrelationships with the tropics. Coherence between the southeastern region and either of the tropical data sets does not exceed the 95% critical value in the interannual frequency band. Coherence is, however, significant at this level between the tropical data sets and those points in the southeastern region which are adjacent to the North American coast. North of 35N the coherence on interannual time scales between grid points adjacent to the west coast of North America and Puerto Chicama SST are generally below the 95% critical value. A similar conclusion has been drawn from lagged cross-correlation studies of temperature and sea level at shore stations along the west coasts of North and South

America by Enfield and Allen (1980). These authors infer from the observed lag of temperature variations behind sea-level variations that "an advective phenomenon perhaps associated with atmospheric teleconnections" may be influencing coastal SST along the California coast. The present study emphasizes the coastal nature of the association between SST in the southeastern region and SST in the eastern equatorial Pacific off Peru.

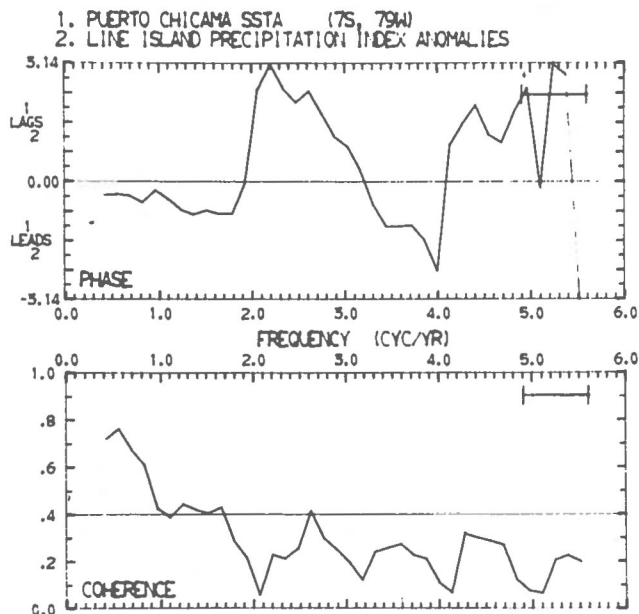


Fig. 37 Coherence and phase estimates between Puerto Chicama SST departures and Line Islands precipitation index departures from mean monthly mean for period 1947-1975. Estimates obtained by five-point frequency smoothing of ensemble averaged estimates from four blocks of 87 months.

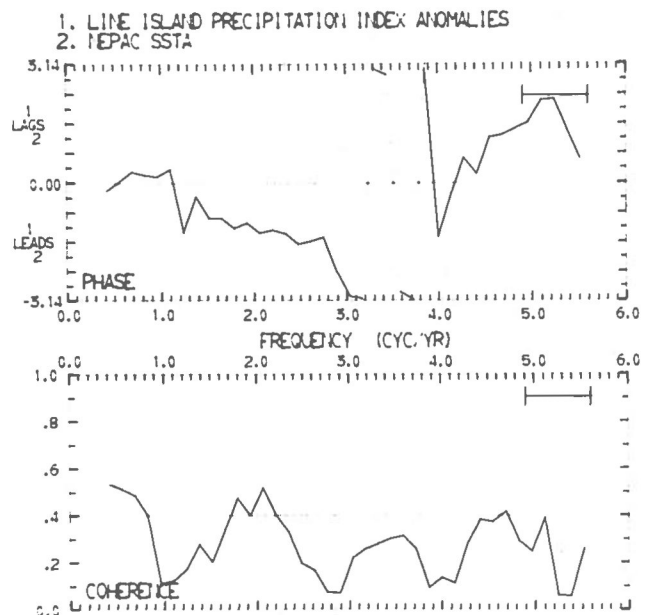


Fig. 38 Coherence and phase estimates between Line Islands precipitation index departures from mean monthly means for period 1947-1975 and SSTA averaged over the Northeastern North Pacific area defined in Fig. 23. Estimates obtained from five-point smoothing of ensemble averaged estimates from four blocks of 87 months.

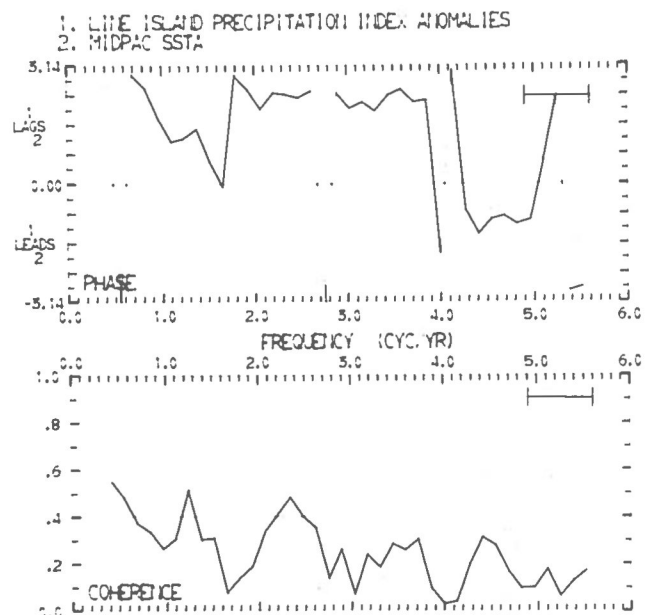


Fig. 39 As in Fig. 38, but for Central North Pacific area defined in Fig. 22.

The results of cross-spectral analysis of temporal variations of SST in the Southwestern North Pacific region (Fig. 25) and the above mentioned tropical data sets are shown in Figs. 40 and 41. Here coherence above the 95% critical value is apparent for periods greater than two years. The associated phase shifts show both Puerto Chicama SST and the Line Islands precipitation index variations leading by approximately  $0.5\pi$  radians. This is roughly the same phase shift seen in Fig. 32 between the northeastern and the southwestern region. Assuming a time scale of these coherent variations of two years, this phase shift translates into a time lag of six months of southwestern variations over those in the Eastern North

Pacific and in the tropics. If taken at face value these results would suggest that oceanic processes might link SST variations in the southwestern region to those identified above in the tropics and midlatitudes.

## V SUMMARY AND DISCUSSION

This report has described some of the results and conclusions drawn from grid point cross-spectral study of spatial and temporal relationships in the 32-year Scripps monthly mean North Pacific SST record. As with all auto- or cross-spectral studies of climatological records of fixed length, the signal associated with potentially interesting properties will be detectable only if it is sufficiently strong relative to the noise associated with uninteresting processes. The present study shows that broadband relationships between spatially separated SSTA variations on interannual time scales can be identified from cross-spectral estimates having approximately 40 degrees of freedom and bandwidth of approximately  $0.75 \text{ yr}^{-1}$ .

The study of local covariance structure and its variation over the North Pacific basin reveals several features which can be qualitatively related to SST forcing mechanisms. First it is clear that coherence on interannual time scales decreases most slowly with increasing separation between the data pair when this separation occurs along the axis of the currents making up the subtropical and subarctic gyres of the North Pacific. The associated phase estimates suggest that advection in these currents may have a slight but detectable influence on the local evolution of sea surface temperature anomalies. More important factors in SST evolution are likely to be the fluctuations in the persistent wind systems which drive the circulation in the gyres since SST anomalies are coherent with nearly no phase shift over distances too large to be connected primarily by advective effects. On the other hand, regions in which coherence on interannual time scales decreases most rapidly with increasing separation are those underlying transition zones between the persistent atmospheric wind systems which by their nature are subjected to pronounced seasonal changes in the overlying wind fields. The role of oceanic processes other than advection in forcing SST changes is most plausibly seen in the Kuroshio extension where relatively large coherence estimates on interannual time scales between meridionally separated pairs on 35N and 45N give way to relatively small estimates on shorter time scales. Similar behavior is seen in estimates for pairs separated zonally by  $20^\circ$  longitude along 40N in the Kuroshio extension. Similar coherence estimates in this longitude sector along 35N and 45N appear to decrease less rapidly with increasing frequency.

There is a tendency for the regions having significant coherence on interannual time scales at relatively large separations to coincide with those regions in which Reynolds (1978) finds the stochastic local SSTA forcing model of Frankignoul and Hasselmann (1977) to be unacceptable. This tendency is particularly marked in the northwestern and southeastern portions of the North Pacific basin. Significant improvements in the representation of physical processes in auto- and cross-spectral models are needed if sharp physical insight is to be drawn from such empirical studies. The dependence of SSTA forcing and

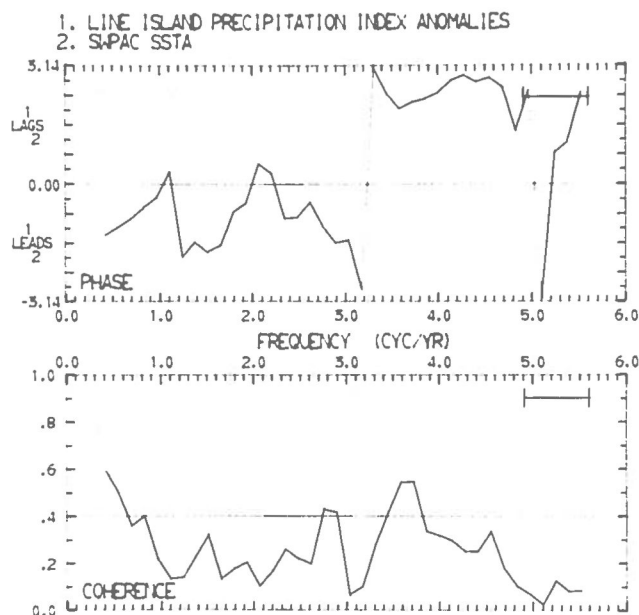


Fig. 40 As in Fig. 38, but for Southwestern North Pacific area defined in Fig. 25.

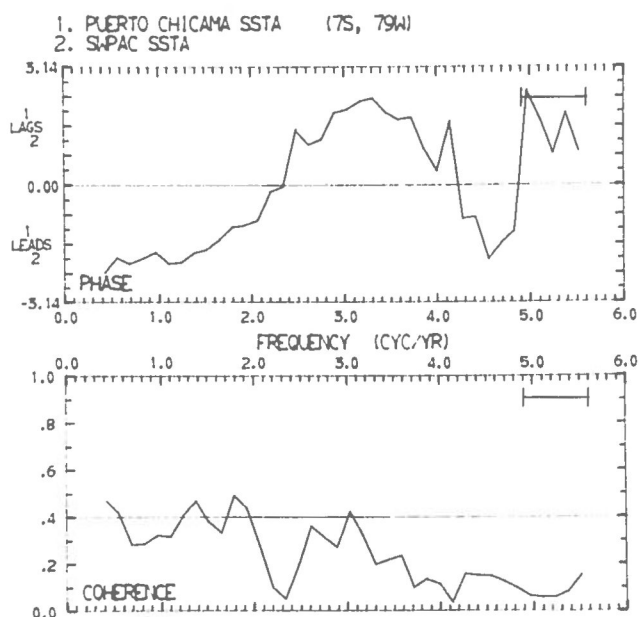


Fig. 41 As in Fig. 35, but for Southwestern North Pacific area defined in Fig. 25.



response on season should be specifically included - particularly if processes influencing SSTA evolution on time scales shorter than one year are to be understood.

As cross-spectral estimates for pairs having separations larger than those of the "local study" are considered, new relationships appear which are strikingly different. Coherence estimates increase with increasing separation along certain lines and marked phase shifts are apparent. Such relationships are most simply interpreted as due to the influence on SST of coherent fluctuations in the spatially inhomogeneous forcing fields associated with large-scale, time mean inhomogeneities of atmospheric and oceanic circulation. Such large-scale structures present on interannual time scales in the SSTA field are logical focal points for investigations of the atmosphere-ocean interaction on interannual time scales.

The pattern of spatial covariation on interannual time scales which emerges from cross-spectral analysis is, on the whole, quite similar to that depicted in the principal EOF's of Pacific SSTA presented by Davis (1976) and Weare et al. (1976). The similarity between estimated coherence contours and the amplitude contours of the first EOF suggests that the large-scale structure of interannual variations in SSTA east of 180W can be viewed as a combination of a signal, represented by temporal variations in the amplitude of the first EOF component alone, superimposed on a noise background which is spatially incoherent at the large scales.

The most obvious candidates for the force generating the signal are the atmospheric variations apparent in the principal EOF pattern of sea-level pressure anomalies which Davis (1976) has shown to be significantly correlated with the principal EOF of SSTA. Advection is probably not responsible for the coherence between central and eastern regions since phase estimates in higher frequency bands, where coherence is significant, appear to be approximately  $\pi$  radians as well. The question of whether the SSTA variation characterized by this large-scale structure is merely a passive response to independent atmospheric fluctuations or whether it is, in any significant way, the result of mutual interaction with the atmosphere is a complicated question requiring further study (Davis, 1978).

The studies of coherence and phase estimates involving the central and northeastern North Pacific SSTA and points in the southwestern North Pacific along 20N and 25N between 145E and 175E reveal significant coherence on interannual time scales. This connection is somewhat unexpected on the basis of the principal EOF pattern for SSTA due to its small amplitude in the southwestern North Pacific. The small amplitude is, no doubt, the EOF manifestation of the apparent phase shift seen here between the southwestern region and the regions to the north and east. The physical basis is unclear for the apparent associations involving the southwestern North Pacific. It has been observed that the subtropical oceanic front existing in this region shows significant interannual intensity variations in apparent concert with transport fluctuations in other branches of the mean circulation (White et al., 1978). Further study of these apparent regional relations may provide further insight into relationships among atmospheric variations, current transport fluctuations and mixed layer thermal anomalies such as those proposed by Reiter (1979).

Cross-spectral analysis further reveals significant coherence on interannual time scales between

regionally averaged North Pacific SST anomalies and two data sets from the Eastern Equatorial Pacific depicting atmospheric and oceanic variations associated with the Southern Oscillation and El Niño. SST anomalies at Puerto Chicama have a slight phase lead over SST anomalies in the Northeastern Pacific and are nearly  $\pi$  radians out of phase with those in Central North Pacific region. These phase relations are quite nearly those to be expected between the three regions of maximum pattern amplitude in the principal nonseasonal EOF of Pacific SST computed by Weare et al. (1976). Their opinion that this eigenvector pattern portrays the North Pacific extension of the El Niño phenomenon is thus supported by the direct analysis of North Pacific SST variations described above. Similar results obtained when Puerto Chicama SSTA is replaced with the time series of the Line Islands precipitation index whose variations Reiter (1978) has shown to be closely associated with anomalies in the convergence of Pacific trade-wind systems in the intertropical convergence zone (ITCZ). It seems likely that the observed coherence on interannual time scales between the tropical and midlatitude data sets and even the relationships among the North Pacific SST regions are related to the Southern Oscillation.

Visual comparison of the time series of coefficients of the principal nonseasonal Pacific sea surface temperature EOF (Weare et al., 1976) with indicators of the Southern Oscillation suggest that cross-spectral analysis of such relationships would reveal significant coherence on interannual time scales. It is less clear that coherence significant at the same level would be revealed between Southern Oscillation indices and the variations in the amplitude of the principal EOF of sea level pressure over the North Pacific (Davis, 1976). If it is not, then the importance of the oceanic mixed layer as a low-pass filter revealing low frequency signals in atmospheric variability is clearly indicated. A better understanding of the characteristics of this filter will be obtained through seasonally stratified studies of the interrelationships seen here and through further analysis of the relationships between SST and relevant properties of the overlying atmosphere.

Finally, the significant connection of tropical circulation phenomena, such as the Southern Oscillation to the North Pacific SST distribution described here, should be considered in the design of studies of the response of atmospheric general circulation models to the SST distribution. Clearly the steady state circulation statistics achieved by a model may be realistic only if both tropical and midlatitude SST distributions are compatibly specified.

## REFERENCES

- Barnett, T.P., 1977: The principal time and space scales of the Pacific trade wind fields. J. Atmos. Sci., **34**, 221-236.
- and R.W. Preisendorfer, 1978: Multifield analog prediction of short-term climate fluctuations using a climate state vector. J. Atmos. Sci., **35**, 1771-1787.
- Bendat, J.S. and A.G. Piersol, 1971: Random data: Analysis and measurement procedures. Wiley-Interscience.
- Bjerknes, S., 1966: A possible response of the atmospheric Hadley circulation to equatorial anomalies in ocean temperature. Tellus, **18**, 820-829.
- , 1969: Atmospheric teleconnections from the equatorial Pacific. Mon. Wea. Rev., **97**, 163-172.
- Bloomfield, P., 1976: Fourier analysis of time series: An introduction. John Wiley and Sons.
- Craddock, J., 1973: Problems and Prospects of eigenvector analysis in meteorology. The Statistician, **22**, 133-143.
- Davis, R.E. 1976: Predictability of sea-surface temperatures and sea level pressure anomalies over the North Pacific Ocean. J. Phys. Oceanogr., **6**, 249-266.
- , 1978: Predictability of sea level pressure anomalies over the North Pacific Ocean. J. Phys. Oceanogr., **8**, 233-246.
- Enfield, D. and J. Allen, 1980: On the structure and dynamics of monthly mean sea level anomalies along the Pacific coast of North and South America. J. Phys. Oceanogr., **10**, 557-578.
- Favorite, F. and D. McLain, 1973: Coherence in trans-pacific movements of positive and negative anomalies of sea-surface temperature, 1953-60. Nature, **244**, 139-143.
- Frankignoul, C. and K. Hasselmann, 1977: Stochastic climate models, Part II: Application to sea-surface temperature anomalies and thermocline variability. Tellus, **29**, 289-305.
- Julian, P.R., 1971: Some aspects of variance spectra of synoptic scale tropospheric wind components in midlatitudes and in the tropics. Mon. Wea. Rev., **99**, 954-965.
- and R. Chervin, 1978: A study of the southern oscillation and Walker circulation phenomenon. Mon. Wea. Rev., **106**, 1433-1451.
- Koopmans, L.H., 1974: The spectral analysis of time series. Academic Press.
- Lorenz, E., 1956: Empirical orthogonal functions and statistical weather prediction. Sci. Rept. No. 1, Statistical Forecasting Project, Dept. of Meteorology, Massachusetts Institute of Technology.
- Namias, J., 1976: Some statistical and synoptic characteristics associated with El Nino. J. Phys. Oceanogr., **6**, 130-138.
- , 1978: Multiple causes of the North American abnormal winter 1976-77. Mo. Wea. Rev., **106**, 279-295.
- Naval Oceanographic office, 1969: Monthly charts of mean, minimum and maximum sea surface temperature of the North Pacific ocean. Naval Oceanographic Office, SP-123.
- Preisendorfer, R. and T. Barnett, 1977: Significance tests for empirical orthogonal functions. Preprints Fifth Conf. Probability and Statistics, Las Vegas, Amer. Met. Soc., 169-172.
- Reiter, E.R., 1978: Long-term wind variability in the tropical Pacific, its possible causes and effects. Mon. Wea. Rev., **106**, 324-330.
- , 1979: Some mechanisms affecting sea-surface temperature anomaly formation in the North Pacific. Arch. Met. Geoph. Biok., Ser. A, **28**, 195-210.
- Reynolds, R.W. 1978: Sea-surface temperature anomalies in the North Pacific Ocean. Tellus, **30**, 97-103.
- Roden, G.I., 1975: On North Pacific temperature, salinity, sound velocity and density fronts and their relation to the wind and energy flux fields. J. Phys. Oceanogr., **5**, 557-571.
- Rogers, J. and H. van Loon, 1979: The seesaw in winter temperatures between Greenland and Northern Europe. Part II: Some oceanic and atmospheric effects in middle and high latitudes. Mon. Wea. Rev., **107**, 509-519.
- U.S. Navy, 1956: Marine climate atlas of the world. Vol. II, North Pacific Ocean. U.S. Government Printing Office.
- van Loon, H. and J. Rogers, 1978: The seesaw in winter temperatures in between Greenland and Northern Europe. Part I: General Description. Mon. Wea. Rev., **106**, 296-310.
- Weare, B., 1977: Empirical orthogonal analysis of Atlantic ocean surface temperatures. Quart. J. R. Met. Soc., **103**, 467-478.
- , A. Navato and R. Newell, 1976: Empirical orthogonal analysis of Pacific sea surface temperatures. J. Phys. Oceanogr., **6**, 671-678.
- White, W.B., 1977: Secular variability in the baroclinic structure of the interior of the North Pacific from 1950-1970. J. Mar. Res., **35**, 587-607.
- , K. Hasunema and H. Solomon, 1978: Large-scale seasonal and secular variability of the subtropical front in the western North Pacific from 1954 to 1974. J. Geophys. Res., **83**, 928-933.
- Willebrand, J., 1978: Temporal and spatial scales of the wind field over the North Pacific and North Atlantic. J. Phys. Oceanogr., **8**, 1080-1094.
- Wyrtki, K. and G. Meyers, 1975: The trade wind field over the Pacific ocean. Part I: The mean field and the mean annual variation. Hawaii Institute of Geophysics Report, HIG 75-1.

Author: John W. Middleton

551.526.6

A CROSS-SPECTRAL STUDY OF THE SPATIAL  
RELATIONSHIPS IN THE NORTH PACIFIC SEA-  
SURFACE TEMPERATURE ANOMALY FIELD

Colorado State University  
Department of Atmospheric Science

Environmental Research Paper No. 23  
March 1980. 25 pp.

U.S. Department of Energy  
Contract DE-AS02-76EV01340  
National Science Foundation  
Grant ATM78-17835

Subject Headings

SST Anomaly Patterns  
Air-Sea Interaction  
Tropical-Midlatitude  
Teleconnections  
Cross-Spectral Analysis of  
Gridded Data Field

Cross-spectral analysis is used to examine the dependence of the temporal covariation of sea-surface temperature (SST) anomalies at pairs of spatially separated points in the North Pacific on (1) the time scale of the variations, (2) the relative displacement of the points and (3) their location within the North Pacific basin. Spatial scales considered here range from 1000 kilometers up to the width of the basin. The study focuses on cross-spectral estimates for the interannual frequency band,  $0.125-0.75 \text{ yr}^{-1}$  although estimates for three other bands spanning higher frequencies are also examined.

Author: John W. Middleton

551.526.6

A CROSS-SPECTRAL STUDY OF THE SPATIAL  
RELATIONSHIPS IN THE NORTH PACIFIC SEA-  
SURFACE TEMPERATURE ANOMALY FIELD

Colorado State University  
Department of Atmospheric Science

Environmental Research Paper No. 23  
March 1980. 25 pp.

U.S. Department of Energy  
Contract DE-AS02-76EV01340  
National Science Foundation  
Grant ATM78-17835

Subject Headings

SST Anomaly Patterns  
Air-Sea Interaction  
Tropical-Midlatitude  
Teleconnections  
Cross-Spectral Analysis of  
Gridded Data Field

Cross-spectral analysis is used to examine the dependence of the temporal covariation of sea-surface temperature (SST) anomalies at pairs of spatially separated points in the North Pacific on (1) the time scale of the variations, (2) the relative displacement of the points and (3) their location within the North Pacific basin. Spatial scales considered here range from 1000 kilometers up to the width of the basin. The study focuses on cross-spectral estimates for the interannual frequency band,  $0.125-0.75 \text{ yr}^{-1}$  although estimates for three other bands spanning higher frequencies are also examined.

Author: John W. Middleton

551.526.6

A CROSS-SPECTRAL STUDY OF THE SPATIAL  
RELATIONSHIPS IN THE NORTH PACIFIC SEA-  
SURFACE TEMPERATURE ANOMALY FIELD

Subject Headings

SST Anomaly Patterns  
Air-Sea Interaction  
Tropical-Midlatitude  
Teleconnections  
Cross-Spectral Analysis of  
Gridded Data Field

Colorado State University  
Department of Atmospheric Sciences

Environmental Research Paper No. 23  
March 1980. 25 pp.

U.S. Department of Energy  
Contract DE-AS02-76EV01340

National Science Foundation  
Grant ATM78-17835

Cross-spectral analysis is used to examine the dependence of the temporal covariation of sea-surface temperature (SST) anomalies at pairs of spatially separated points in the North Pacific on (1) the time scale of the variations, (2) the relative displacement of the points and (3) their location within the North Pacific basin. Spatial scales considered here range from 1000 kilometers up to the width of the basin. The study focuses on cross-spectral estimates for the interannual frequency band,  $0.125-0.75 \text{ yr}^{-1}$  although estimates for three other bands spanning higher frequencies are also examined.

Author: John W. Middleton

551.526.6

A CROSS-SPECTRAL STUDY OF THE SPATIAL  
RELATIONSHIPS IN THE NORTH PACIFIC SEA-  
SURFACE TEMPERATURE ANOMALY FIELD

Subject Headings

SST Anomaly Patterns  
Air-Sea Interaction  
Tropical-Midlatitude  
Teleconnections  
Cross-Spectral Analysis of  
Gridded Data Field

Colorado State University  
Department of Atmospheric Science

Environmental Research Paper No. 23  
March 1980. 25 pp.

U.S. Department of Energy  
Contract DE-AS02-76EV01340

National Science Foundation  
Grant ATM78-17835

Cross-spectral analysis is used to examine the dependence of the temporal covariation of sea-surface temperature (SST) anomalies at pairs of spatially separated points in the North Pacific on (1) the time scale of the variations, (2) the relative displacement of the points and (3) their location within the North Pacific basin. Spatial scales considered here range from 1000 kilometers up to the width of the basin. The study focuses on cross-spectral estimates for the interannual frequency band,  $0.125-0.75 \text{ yr}^{-1}$  although estimates for three other bands spanning higher frequencies are also examined.

The study shows that, on interannual time scales, zonal and meridional coherence length scales are largest along the axes of the major mean North Pacific currents comprising the subtropical and subarctic gyres. The associated phase estimates uniformly indicate a small phase lead for the upstream point. These phase shifts appear to be relatively independent of separation within these regions suggesting that large-scale atmospheric forcing rather than advection is primarily responsible for the observed coherence.

The out-of-phase relationship found between variations in the central North Pacific and those off the west coast of North America confirms the pattern appearing in the principal empirical orthogonal function of the sea-surface temperature anomaly field. Both of these regions are significantly coherent on interannual time scales with those in the southwestern North Pacific. Phase estimates show the variations in the southwestern region to have an apparent phase lag of  $\pi/4$  to  $\pi/2$  radians relative to those in the other regions.

Cross-spectral analysis of the relationships between SST variations in these areas and at Puerto Chicama, Peru reveals significant coherence on interannual time scales. The associated phase estimates show variations in the Northeastern North Pacific to have a slight lag behind those at Puerto Chicama while SST variations in the Central North Pacific are shifted by approximately  $\pi$  radians relative to those at Puerto Chicama. The hypothesis is advanced that the tropical-midlatitude teleconnection Bjerknes associated with the Southern Oscillation and El Niño is thus revealed in the low-pass filtered response of mid-latitude SST to atmospheric forcing.

The study shows that, on interannual time scales, zonal and meridional coherence length scales are largest along the axes of the major mean North Pacific currents comprising the subtropical and subarctic gyres. The associated phase estimates uniformly indicate a small phase lead for the upstream point. These phase shifts appear to be relatively independent of separation within these regions suggesting that large-scale atmospheric forcing rather than advection is primarily responsible for the observed coherence.

The out-of-phase relationship found between variations in the central North Pacific and those off the west coast of North America confirms the pattern appearing in the principal empirical orthogonal function of the sea-surface temperature anomaly field. Both of these regions are significantly coherent on interannual time scales with those in the southwestern North Pacific. Phase estimates show the variations in the southwestern region to have an apparent phase lag of  $\pi/4$  to  $\pi/2$  radians relative to those in the other regions.

Cross-spectral analysis of the relationships between SST variations in these areas and at Puerto Chicama, Peru reveals significant coherence on interannual time scales. The associated phase estimates show variations in the Northeastern North Pacific to have a slight lag behind those at Puerto Chicama while SST variations in the Central North Pacific are shifted by approximately  $\pi$  radians relative to those at Puerto Chicama. The hypothesis is advanced that the tropical-midlatitude teleconnection Bjerknes associated with the Southern Oscillation and El Niño is thus revealed in the low-pass filtered response of mid-latitude SST to atmospheric forcing.

The study shows that, on interannual time scales, zonal and meridional coherence length scales are largest along the axes of the major mean North Pacific currents comprising the subtropical and subarctic gyres. The associated phase estimates uniformly indicate a small phase lead for the upstream point. These phase shifts appear to be relatively independent of separation within these regions suggesting that large-scale atmospheric forcing rather than advection is primarily responsible for the observed coherence.

The out-of-phase relationship found between variations in the central North Pacific and those off the west coast of North America confirms the pattern appearing in the principal empirical orthogonal function of the sea-surface temperature anomaly field. Both of these regions are significantly coherent on interannual time scales with those in the southwestern North Pacific. Phase estimates show the variations in the southwestern region to have an apparent phase lag of  $\pi/4$  to  $\pi/2$  radians relative to those in the other regions.

Cross-spectral analysis of the relationships between SST variations in these areas and at Puerto Chicama, Peru reveals significant coherence on interannual time scales. The associated phase estimates show variations in the Northeastern North Pacific to have a slight lag behind those at Puerto Chicama while SST variations in the Central North Pacific are shifted by approximately  $\pi$  radians relative to those at Puerto Chicama. The hypothesis is advanced that the tropical-midlatitude teleconnection Bjerknes associated with the Southern Oscillation and El Niño is thus revealed in the low-pass filtered response of mid-latitude SST to atmospheric forcing.

The study shows that, on interannual time scales, zonal and meridional coherence length scales are largest along the axes of the major mean North Pacific currents comprising the subtropical and subarctic gyres. The associated phase estimates uniformly indicate a small phase lead for the upstream point. These phase shifts appear to be relatively independent of separation within these regions suggesting that large-scale atmospheric forcing rather than advection is primarily responsible for the observed coherence.

The out-of-phase relationship found between variations in the central North Pacific and those off the west coast of North America confirms the pattern appearing in the principal empirical orthogonal function of the sea-surface temperature anomaly field. Both of these regions are significantly coherent on interannual time scales with those in the southwestern North Pacific. Phase estimates show the variations in the southwestern region to have an apparent phase lag of  $\pi/4$  to  $\pi/2$  radians relative to those in the other regions.

Cross-spectral analysis of the relationships between SST variations in these areas and at Puerto Chicama, Peru reveals significant coherence on interannual time scales. The associated phase estimates show variations in the Northeastern North Pacific to have a slight lag behind those at Puerto Chicama while SST variations in the Central North Pacific are shifted by approximately  $\pi$  radians relative to those at Puerto Chicama. The hypothesis is advanced that the tropical-midlatitude teleconnection Bjerknes associated with the Southern Oscillation and El Niño is thus revealed in the low-pass filtered response of mid-latitude SST to atmospheric forcing.

Author: John W. Middleton

551.526.6

A CROSS-SPECTRAL STUDY OF THE SPATIAL  
RELATIONSHIPS IN THE NORTH PACIFIC SEA-  
SURFACE TEMPERATURE ANOMALY FIELD

Colorado State University  
Department of Atmospheric Science

Environmental Research Paper No. 23  
March 1980. 25 pp.

U.S. Department of Energy  
Contract DE-AS02-76EV01340

National Science Foundation  
Grant ATM78-17835

Subject Headings

SST Anomaly Patterns  
Air-Sea Interaction  
Tropical-Midlatitude  
Teleconnections  
Cross-Spectral Analysis of  
Gridded Data Field

Cross-spectral analysis is used to examine the dependence of the temporal covariation of sea-surface temperature (SST) anomalies at pairs of spatially separated points in the North Pacific on (1) the time scale of the variations, (2) the relative displacement of the points and (3) their location within the North Pacific basin. Spatial scales considered here range from 1000 kilometers up to the width of the basin. The study focuses on cross-spectral estimates for the interannual frequency band,  $0.125\text{--}0.75\text{ yr}^{-1}$  although estimates for three other bands spanning higher frequencies are also examined.

Author: John W. Middleton

551.526.6

A CROSS-SPECTRAL STUDY OF THE SPATIAL  
RELATIONSHIPS IN THE NORTH PACIFIC SEA-  
SURFACE TEMPERATURE ANOMALY FIELD

Colorado State University  
Department of Atmospheric Science

Environmental Research Paper No. 23  
March 1980. 25 pp.

U.S. Department of Energy  
Contract DE-AS02-76EV01340

National Science Foundation  
Grant ATM78-17835

Subject Headings

SST Anomaly Patterns  
Air-Sea Interaction  
Tropical-Midlatitude  
Teleconnections  
Cross-Spectral Analysis of  
Gridded Data Field

Cross-spectral analysis is used to examine the dependence of the temporal covariation of sea-surface temperature (SST) anomalies at pairs of spatially separated points in the North Pacific on (1) the time scale of the variations, (2) the relative displacement of the points and (3) their location within the North Pacific basin. Spatial scales considered here range from 1000 kilometers up to the width of the basin. The study focuses on cross-spectral estimates for the interannual frequency band,  $0.125\text{--}0.75\text{ yr}^{-1}$  although estimates for three other bands spanning higher frequencies are also examined.

Author: John W. Middleton

551.526.6

A CROSS-SPECTRAL STUDY OF THE SPATIAL  
RELATIONSHIPS IN THE NORTH PACIFIC SEA-  
SURFACE TEMPERATURE ANOMALY FIELD

Colorado State University  
Department of Atmospheric Science

Environmental Research Paper No. 23  
March 1980. 25 pp.

U.S. Department of Energy  
Contract DE-AS02-76EV01340

National Science Foundation  
Grant ATM78-17835

Subject Headings

SST Anomaly Patterns  
Air-Sea Interaction  
Tropical-Midlatitude  
Teleconnections  
Cross-Spectral Analysis of  
Gridded Data Field

Cross-spectral analysis is used to examine the dependence of the temporal covariation of sea-surface temperature (SST) anomalies at pairs of spatially separated points in the North Pacific on (1) the time scale of the variations, (2) the relative displacement of the points and (3) their location within the North Pacific basin. Spatial scales considered here range from 1000 kilometers up to the width of the basin. The study focuses on cross-spectral estimates for the interannual frequency band,  $0.125\text{--}0.75\text{ yr}^{-1}$  although estimates for three other bands spanning higher frequencies are also examined.

Author: John W. Middleton

551.526.6

A CROSS-SPECTRAL STUDY OF THE SPATIAL  
RELATIONSHIPS IN THE NORTH PACIFIC SEA-  
SURFACE TEMPERATURE ANOMALY FIELD

Colorado State University  
Department of Atmospheric Science

Environmental Research Paper No. 23  
March 1980. 25 pp.

U.S. Department of Energy  
Contract DE-AS02-76EV01340

National Science Foundation  
Grant ATM78-17835

Subject Headings

SST Anomaly Patterns  
Air-Sea Interaction  
Tropical-Midlatitude  
Teleconnections  
Cross-Spectral Analysis of  
Gridded Data Field

Cross-spectral analysis is used to examine the dependence of the temporal covariation of sea-surface temperature (SST) anomalies at pairs of spatially separated points in the North Pacific on (1) the time scale of the variations, (2) the relative displacement of the points and (3) their location within the North Pacific basin. Spatial scales considered here range from 1000 kilometers up to the width of the basin. The study focuses on cross-spectral estimates for the interannual frequency band,  $0.125\text{--}0.75\text{ yr}^{-1}$  although estimates for three other bands spanning higher frequencies are also examined.



The study shows that, on interannual time scales, zonal and meridional coherence length scales are largest along the axes of the major mean North Pacific currents comprising the subtropical and subarctic gyres. The associated phase estimates uniformly indicate a small phase lead for the upstream point. These phase shifts appear to be relatively independent of separation within these regions suggesting that large-scale atmospheric forcing rather than advection is primarily responsible for the observed coherence.

The out-of-phase relationship found between variations in the central North Pacific and those off the west coast of North America confirms the pattern appearing in the principal empirical orthogonal function of the sea-surface temperature anomaly field. Both of these regions are significantly coherent on interannual time scales with those in the southwestern North Pacific. Phase estimates show the variations in the southwestern region to have an apparent phase lag of  $\pi/4$  to  $\pi/2$  radians relative to those in the other regions.

Cross-spectral analysis of the relationships between SST variations in these areas and at Puerto Chicama, Peru reveals significant coherence on interannual time scales. The associated phase estimates show variations in the Northeastern North Pacific to have a slight lag behind those at Puerto Chicama while SST variations in the Central North Pacific are shifted by approximately  $\pi$  radians relative to those at Puerto Chicama. The hypothesis is advanced that the tropical-midlatitude teleconnection Bjerknes associated with the Southern Oscillation and El Niño is thus revealed in the low-pass filtered response of mid-latitude SST to atmospheric forcing.

The study shows that, on interannual time scales, zonal and meridional coherence length scales are largest along the axes of the major mean North Pacific currents comprising the subtropical and subarctic gyres. The associated phase estimates uniformly indicate a small phase lead for the upstream point. These phase shifts appear to be relatively independent of separation within these regions suggesting that large-scale atmospheric forcing rather than advection is primarily responsible for the observed coherence.

The out-of-phase relationship found between variations in the central North Pacific and those off the west coast of North America confirms the pattern appearing in the principal empirical orthogonal function of the sea-surface temperature anomaly field. Both of these regions are significantly coherent on interannual time scales with those in the southwestern North Pacific. Phase estimates show the variations in the southwestern region to have an apparent phase lag of  $\pi/4$  to  $\pi/2$  radians relative to those in the other regions.

Cross-spectral analysis of the relationships between SST variations in these areas and at Puerto Chicama, Peru reveals significant coherence on interannual time scales. The associated phase estimates show variations in the Northeastern North Pacific to have a slight lag behind those at Puerto Chicama while SST variations in the Central North Pacific are shifted by approximately  $\pi$  radians relative to those at Puerto Chicama. The hypothesis is advanced that the tropical-midlatitude teleconnection Bjerknes associated with the Southern Oscillation and El Niño is thus revealed in the low-pass filtered response of mid-latitude SST to atmospheric forcing.

C 2 2

The study shows that, on interannual time scales, zonal and meridional coherence length scales are largest along the axes of the major mean North Pacific currents comprising the subtropical and subarctic gyres. The associated phase estimates uniformly indicate a small phase lead for the upstream point. These phase shifts appear to be relatively independent of separation within these regions suggesting that large-scale atmospheric forcing rather than advection is primarily responsible for the observed coherence.

The out-of-phase relationship found between variations in the central North Pacific and those off the west coast of North America confirms the pattern appearing in the principal empirical orthogonal function of the sea-surface temperature anomaly field. Both of these regions are significantly coherent on interannual time scales with those in the southwestern North Pacific. Phase estimates show the variations in the southwestern region to have an apparent phase lag of  $\pi/4$  to  $\pi/2$  radians relative to those in the other regions.

Cross-spectral analysis of the relationships between SST variations in these areas and at Puerto Chicama, Peru reveals significant coherence on interannual time scales. The associated phase estimates show variations in the Northeastern North Pacific to have a slight lag behind those at Puerto Chicama while SST variations in the Central North Pacific are shifted by approximately  $\pi$  radians relative to those at Puerto Chicama. The hypothesis is advanced that the tropical-midlatitude teleconnection Bjerknes associated with the Southern Oscillation and El Niño is thus revealed in the low-pass filtered response of mid-latitude SST to atmospheric forcing.

The study shows that, on interannual time scales, zonal and meridional coherence length scales are largest along the axes of the major mean North Pacific currents comprising the subtropical and subarctic gyres. The associated phase estimates uniformly indicate a small phase lead for the upstream point. These phase shifts appear to be relatively independent of separation within these regions suggesting that large-scale atmospheric forcing rather than advection is primarily responsible for the observed coherence.

The out-of-phase relationship found between variations in the central North Pacific and those off the west coast of North America confirms the pattern appearing in the principal empirical orthogonal function of the sea-surface temperature anomaly field. Both of these regions are significantly coherent on interannual time scales with those in the southwestern North Pacific. Phase estimates show the variations in the southwestern region to have an apparent phase lag of  $\pi/4$  to  $\pi/2$  radians relative to those in the other regions.

Cross-spectral analysis of the relationships between SST variations in these areas and at Puerto Chicama, Peru reveals significant coherence on interannual time scales. The associated phase estimates show variations in the Northeastern North Pacific to have a slight lag behind those at Puerto Chicama while SST variations in the Central North Pacific are shifted by approximately  $\pi$  radians relative to those at Puerto Chicama. The hypothesis is advanced that the tropical-midlatitude teleconnection Bjerknes associated with the Southern Oscillation and El Niño is thus revealed in the low-pass filtered response of mid-latitude SST to atmospheric forcing.

### Previously Published Environmental Research Papers

- No. 1 On the Variability of Hemispheric Scale Energy Parameters, by J.P. McGuirk, E.R. Reiter and A.M. Barbieri, January 1975.
- No. 2 On Determining Vertical Wind Velocities from Eole Constant-Density Balloon Data, by Robert M. Banta, June 1975.
- No. 3 Atmospheric Eddy Transports and Their Efficiencies, by Srinivasan Srivatsangam, January 1976.
- No. 4 Interannual Variations and Regional Effects of Hemispheric Parameters, by Ann M. Starr (née Barbieri), July 1976.
- No. 5 The Effects of Atmospheric Variability on Energy Utilization and Conservation, by E.R. Reiter et al., November 1976.
- No. 6 Fluctuations in the Atmosphere's Energy Cycle, by James P. McGuirk, March 1977.
- No. 7 Oceanic Latent and Sensible Heat Flux Variability and Air-Interaction, by Anne D. Seigel, April 1977.
- No. 8 Observations of Stratospheric Thermal Structure from Satellites, by Thomas J. Kleespies, May 1977.
- No. 9 Effects of Coal Mine Drainage on Macroinvertebrates of Trout Creek, Colorado, by Steven P. Canton and James V. Ward, April 1977.
- No. 10 Potential Effects of Oil Shale Extraction and Processing Activities on Macroinvertebrates of Piceance and Black Sulphur Creeks, Colorado, by Lawrence J. Gray and James V. Ward, April 1977.
- No. 11 Modeling Atmospheric Dispersion of Lead Particulates From a Highway, by Paul C. Katen, July 1977.
- No. 12 Residence Time of Atmospheric Pollutants and Long-Range Transport, by Teizi Henmi, Elmar R. Reiter and Roger Edson, July 1977.
- No. 13 Quasi-Periodicities of Atmospheric Circulation and Their Application to Long-Range Weather Prediction, by S. Srivatsangam, Chi-Nan Hsiao, and Elmar R. Reiter, November 1977.
- No. 14 The Effects of Atmospheric Variability on Energy Utilization and Conservation, by Elmar R. Reiter, et al., February 1978.
- No. 15 Long-Range Transport and Transformation of SO<sub>2</sub> and Sulfate, by Teizi Henmi and Elmar R. Reiter, September 1978.
- No. 16 The Interannual Variability of Northern Hemisphere Precipitation, by Thomas J. Corona, December 1978.
- No. 17 Interannual Variation of Atmospheric Meridional Eddy Transports, by Chi-Nan Hsiao, April 1979.
- No. 18 The Effects of Atmospheric Variability on Energy Utilization and Conservation, by Elmar R. Reiter, et al., March 1979.
- No. 19 Relationships Between Precipitation, Pressure and Ocean Temperature, by Patrick Allen Haar, June 1979.
- No. 20 Further Investigation of the Interannual Variability of Northern Hemisphere Continental Precipitation, by Thomas J. Corona, August 1979.
- No. 21 On the Dynamic Forcing of Short-Term Climate Fluctuations by Feedback Mechanisms, by Elmar R. Reiter, September 1979.
- No. 22 A Preliminary Study of the Variability in the Frequency of Typhoon Formation Over the West Pacific Ocean, by Yi-Hui Ding and Elmar R. Reiter, June 1980.